Quantum friction on monoatomic layers and its classical analog

Stanislav I. Maslovski and Mário G. Silveirinha
Departamento de Engenharia Electrotécnica, Instituto de Telecomunicações, Universidade de Coimbra, Pólo II, 3030-290 Coimbra, Portugal
(Received 8 February 2013; published 15 July 2013)

We consider the effect of quantum friction at zero absolute temperature resulting from polaritonic interactions in closely positioned two-dimensional arrays of polarizable atoms (e.g., graphene sheets) or thin dielectric sheets modeled as such arrays. The arrays move one with respect to another with a nonrelativistic velocity $v \ll c$. We confirm that quantum friction is inevitably related to material dispersion, and that such friction vanishes in nondispersive media. In addition, we consider a classical analog of the quantum friction which allows us to establish a link between the phenomena of quantum friction and classical parametric generation. In particular, we demonstrate how the quasiparticle generation rate typically obtained from the quantum Fermi golden rule can be calculated classically.

DOI: 10.1103/PhysRevB.88.035427 PACS number(s): 73.61.−r, 73.20.Mf, 68.35.Af

I. INTRODUCTION

The phenomenon of quantum friction[1–6] has attracted a lot of attention recently,[7–22] mostly because of a few "controversies" linked to this effect, especially at temperatures approaching absolute zero. At the macroscopic level, the quantum friction force is commonly perceived as a force exerted on bodies moving in the vicinity of each other, which emerges from the zero-point fluctuations of the electromagnetic field in the space surrounding the bodies. This force acts against the movement of the bodies, and, thus, it is tempting to imagine that there is a certain "viscosity" associated with the fluctuating field[3] that persists even at $T = 0$ K. It was recently found that the normal Casimir forces are also affected by the shear movement of the bodies.[23]

Although this picture is very intuitive, it is not immediately evident how such a *nonreversible* and *nonconservative* effect as friction may result out of the mentioned quantum-mechanical model. Indeed, in quantum electrodynamics it is typically assumed that the fluctuating electromagnetic field, together with the particles that interact with it, is captured within an adiabatically closed cavity. It is evident that within such an environment the quasistationary processes (for instance, slow relative movements of bodies in the cavity which do not destroy the state of thermodynamic equilibrium) are *reversible* at $T = 0$ K, even if large ensembles of particles are involved, simply because the Nernst theorem requires the entropy of the *entire* system to vanish at $T = 0$ K.

There is, however, no such contradiction when one deals with open systems which are *not* in a state of precise equilibrium with their background. In such systems there may exist heat and entropy flows, therefore the extra entropy and heat created locally in a frictive process can be eventually transferred to the environment by some intermediate agents. In the same manner, in this work we understand quantum friction as a dissipative effect resulting from *generation* of excitations (such as plasmons, polaritons, phonons, etc.) that eventually escape the quantum dynamic system (which is otherwise conservative) in one way or another. In lossy media such processes result in generation of heat, however, it is also known that the quantum friction on rotating bodies in vacuum is associated with generation of photons.[21,22]

Here we study the quantum friction between two very thin (monoatomic in the limiting case) moving dispersive dielectric sheets separated by a vacuum gap. To account for the time dispersion we employ a model of discrete oscillators, in which the polarized atoms of a dielectric are represented by oscillating dipoles having a certain resonant frequency and an effective mass. The collective dipole oscillations in a dielectric—the polarization waves whose quanta are designated here (following Ref. 24) by polaritons—are then studied using a Hamiltonian formalism that takes into account the interaction of the dipoles within a sheet (although in our theory we consider only near-range excitations for which one may use nonretarding approximation for the dipole-to-dipole interaction in thin dielectric layers, one may still regard such modes to be a blend of the dipole vibrations and the electromagnetic waves captured within a layer—a property typical for polaritons, as is commonly understood). We quantize the polarization waves separately in the two sheets, while allowing the waves in these sheets to interact. The interaction Hamiltonian of the two sheets is obtained under a nonretarding, nonrelativistic approximation for the electric dipole-to-dipole interaction. When the sheets move, this interaction results in transitions from the ground state of the polarization field of the dielectric sheets to the nearby states, i.e., the relative movement of the sheets generates pairs of polaritons which eventually leave the system (e.g., get absorbed) which results in a friction force exerted on the sheets.

It is important to note that the quantum model that we describe in this work complements the previously available models of quantum friction[4,5,17,18] in continuous media by highlighting the role of material dispersion and clarifying the underlying physical mechanisms of this phenomenon. Even though our theory is based on arrays of discrete oscillators, in our calculations we consider the limit wherein the spacing between the discrete oscillators is infinitesimal. In this limit, from the electromagnetic point of view, the dipole array is equivalent to a perfectly smooth continuous dielectric sheet. Thus, the friction force calculated in this work is not the result of the discreteness of the arrays but rather a consequence of instabilities of electromagnetic field in moving media.

Under this perspective, the effect of quantum friction does not appear significantly different from, for instance, the radiative loss in the Smith-Purcell effect[25] or the stopping power in the Cherenkov effect.[26,27] Moreover, in this work we show that there is not that much *specifically quantum*

in the phenomenon of quantum friction, and that this phenomenon is tightly linked to the classic theories of parametric generation.[28–30] Namely, we show that provided the initial fluctuating field is given, it is possible to calculate using classical arguments the growth rate of these fluctuations and the rate of generation of polaritonic energy. As is shown in Sec. V, the result of such classical calculation coincides with the quantum-mechanical calculation of the quasiparticle generation rate. Moreover, under certain assumptions, the friction force calculated classically coincides with the one calculated quantum mechanically if one regards the zero-point fluctuations as the initial "source" of the fluctuating field at $T = 0$. Such a point of view is consistent with explanations of the quantum friction effect as a result of the interaction between charge density fluctuations in moving bodies.[4–6]

Before going into details, we have to note also that a related model of quantum friction was previously developed by Pendry[8] for the special case of plasmons in metals with Drude-type dispersion with negligible loss. In Pendry's case the phase velocity of short-wavelength plasmons supported by the metal slabs approaches $v_{\rm ph} = \omega_{\rm p}/k$, where $\omega_{\rm p}$ is the plasma frequency and k is the plasmon propagation factor. A very important point not discussed by Pendry is that for plasmons with very short wavelength the phase velocity can be arbitrarily low. In particular, at some k, $v_{\rm ph}$ can become much lower than the velocity of the relative movement of the slabs. However, within the framework of this paper, it is immediately understood that such a situation may lead to instabilities analogous to the instabilities in moving media above the threshold of the Cherenkov effect.[31] Such instabilities in turn lead to generation of radiation, which in the end gives rise to quantum friction (for the behavior of the normal Casimir forces at the threshold of the Cherenkov effect see Ref. 32). A widely adopted explanation of the quantum friction phenomenon pictures it as a result of asymmetry in reflections of photons by moving dielectric slabs.[4] This explanation can be found in many semiclassical works on quantum friction, and is very different from the picture that emerges from our theory.

In this work we also prove quantum mechanically that in dense arrays of nondispersive dipolar oscillators the effect of quantum friction completely disappears at nonrelativistic velocities $v \ll c$, even though the dipoles in the two moving arrays still respond to the electric field and interact electromagnetically. It must be noted that in the related quantum-mechanical plasmon-based model of Ref. 8 the limit of no dispersion ($\omega_{\rm p} \to 0$) coincides with the limit $\varepsilon_{\rm r} = 1 - \omega_{\rm p}^2/\omega^2 \to 1$, in which the dielectric response of the material vanishes. In contrast, in our framework we may remove the dispersion by letting the resonant frequency of the dipole vibrations approach infinity, while keeping the static polarizability of the dipoles constant and greater than zero.

II. HAMILTONIAN FORMALISM AND QUANTIZATION OF POLARIZATION WAVES IN A THIN DIELECTRIC SLAB

Here we are going to consider collective oscillations of the bounded electrons in a thin dispersive dielectric slab of infinite extent, i.e., the polarization waves of such a slab. Classically, such modes are guided waves supported by a dielectric slab in the case when electrostatic interaction between polarized atoms remains dominant even on the scale of a wavelength. These modes split into dispersion branches characterized by polarization direction and distribution of the polarization across the slab. In thin dielectric sheets, the modes with less variation across the sheet are the ones mostly excited. Although it is possible to develop a formulation in which all the normal modes are taken into account, in what follows we focus only on the dominant modes. This allows us to approximate a thin dielectric sheet by a planar array of oscillators. Physically, in this model the oscillating electrons in a vicinity of a given line across a dielectric sheet appear strongly coupled, so that the dynamics of such a line of oscillators is described with just a single effective oscillator, characterized by an effective mass and a resonant frequency. The same model can be applied without approximation to real two-dimensional structures, for example, to graphene sheets or other monoatomic or monomolecular layers.

Nonrelativistic Hamiltonian dynamics of bounded electrons in a thin dielectric slab is formulated and discussed in Appendix A. Based on these findings, the Hamiltonian of such a slab modeled as an array of effective dipolar oscillators can be written as

$$H = \frac{1}{2}\sum_s \Bigg[\mathbf{x}_s \cdot \left(m_{\mathrm{eff},\perp}\Omega_\perp^2 \bar{\bar{\mathbf{I}}}_\perp + m_{\mathrm{eff},\parallel}\Omega_\parallel^2 \bar{\bar{\mathbf{I}}}_\parallel \right) \cdot \mathbf{x}_s + \mathbf{p}_s \cdot \left(m_{\mathrm{eff},\perp}^{-1} \bar{\bar{\mathbf{I}}}_\perp + m_{\mathrm{eff},\parallel}^{-1} \bar{\bar{\mathbf{I}}}_\parallel \right) \cdot \mathbf{p}_s + \frac{e^2}{4\pi\varepsilon_0} \sum_{q\neq s} \mathbf{x}_s \cdot \bar{\bar{\bar{\Phi}}}_{sq} \cdot \mathbf{x}_q \Bigg], \tag{1}$$

where $\mathbf{x}_s = \mathbf{x}_{s,\perp} + \mathbf{x}_{s,\parallel}$, $\mathbf{p}_s = \mathbf{p}_{s,\perp} + \mathbf{p}_{s,\parallel}$, with $\mathbf{x}_{s,\perp}$ and $\mathbf{x}_{s,\parallel}$ being the effective charge displacements in these oscillators across and along the array plane, respectively, and $\mathbf{p}_{s,\perp}$ and $\mathbf{p}_{s,\parallel}$ being the conjugate momenta associated with them. The parameters $m_{\mathrm{eff},\perp}$, $\Omega_\perp$ and $m_{\mathrm{eff},\parallel}$, $\Omega_\parallel$ are the effective oscillator parameters for the two types of oscillations (see Appendix A). The dyadics $\bar{\bar{\mathbf{I}}}_\perp$ and $\bar{\bar{\mathbf{I}}}_\parallel$ are the out-of-plane and in-plane unity dyadics, respectively, and the interaction dyadic $\bar{\bar{\bar{\Phi}}}_{sq}$ is defined as

$$\bar{\bar{\bar{\Phi}}}_{sq} = \frac{\bar{\bar{\mathbf{I}}} - 3\mathbf{u}_{sq}\mathbf{u}_{sq}}{R_{sq}^3}, \tag{2}$$

where $\bar{\bar{\mathbf{I}}} = \bar{\bar{\mathbf{I}}}_\perp + \bar{\bar{\mathbf{I}}}_\parallel$ represents the identity dyadic. In Eqs. (1) and (2) the indices s and q run over the effective oscillators, with $\mathbf{R}_{sq} = \mathbf{u}_{sq}R_{sq}$ being the radius vector from the sth oscillator to the qth oscillator.

Although Eq. (1) associates only a pair of characteristic frequencies ($\Omega_\perp$ and $\Omega_\parallel$) with the electron oscillations in the slab, the quantum theory that we develop next is not limited by this fact, and is readily generalizable to dielectrics with multiresonant response. In fact, the Hamiltonian of an ensemble of coupled oscillators can be also represented more generally as

$$H = \frac{1}{2}\sum_{m,n}\left(\frac{\partial^2 H}{\partial x_m \partial x_n} x_m x_n + \frac{\partial^2 H}{\partial p_m \partial p_n} p_m p_n \right), \tag{3}$$

where x_m are the independent degrees of freedom (three per each oscillator) and p_m are their conjugate momenta. The dynamic equations for such a system can be written in the block matrix notation as

$$i\frac{d}{dt}\underbrace{\begin{pmatrix}[x_m]_K\\ [p_m]_K\end{pmatrix}}_{\mathbf{F}} = \underbrace{\begin{pmatrix}0 & i\\ -i & 0\end{pmatrix}}_{\mathbf{J}} \cdot \underbrace{\begin{pmatrix}\left[\frac{\partial^2 H}{\partial x_m \partial x_n}\right]_{K\times K} & 0\\ 0 & \left[\frac{\partial^2 H}{\partial p_m \partial p_n}\right]_{K\times K}\end{pmatrix}}_{\mathbf{M}} \cdot \underbrace{\begin{pmatrix}[x_n]_K\\ [p_n]_K\end{pmatrix}}_{\mathbf{F}}, \tag{4}$$

with K being the total number of the degrees of freedom, and $i=\sqrt{-1}$. The representation (4) allows us to introduce a basis in the space of state vectors $\mathbf{F}$ and diagonalize the system (4) using an approach consistent with Ref. 33. Indeed, because the matrix $\mathbf{M}$ of the positive definite quadratic form (3) is symmetric and real valued, the same matrix is positive definite in the space of complex vectors, and, thus, we may define a weighted inner product $\langle \mathbf{F}_1|\mathbf{F}_2\rangle \equiv \mathbf{F}_1^\dagger \mathbf{M}\mathbf{F}_2$, where † denotes the conjugate transpose (adjoint) operation. Next, because $\mathbf{M}$ and $\mathbf{J}$ are self-adjoint matrices, we have $\langle \mathbf{J}\mathbf{M}\mathbf{F}_1|\mathbf{F}_2\rangle = (\mathbf{J}\mathbf{M}\mathbf{F}_1)^\dagger \mathbf{M}\mathbf{F}_2 = \langle \mathbf{F}_1|\mathbf{J}\mathbf{M}\mathbf{F}_2\rangle$, and, thus, the matrix $\mathbf{J}\mathbf{M}$ defines a Hermitian operator in the inner product space defined above. Therefore, the eigenvectors of this operator form an orthogonal basis $\mathbf{F}_\mathbf{k}$, which can be made orthonormal: $\langle \mathbf{F}_\mathbf{k}|\mathbf{F}_\mathbf{k}\rangle = 1$. The eigenvalues $\omega_\mathbf{k}$ of this operator are real valued. Moreover, it is trivial to see that any eigenvector $\mathbf{F}_\mathbf{k}$ with $\omega_\mathbf{k} > 0$ is accompanied by the eigenvector $\mathbf{F}_\mathbf{k}^*$ with the eigennumber $-\omega_\mathbf{k} < 0$.

In Appendix B we obtain the spectrum of this operator and prove that in isotropic (e.g., square or hexagonal) dense lattices the complete phase vector space can be split into three independent subspaces: $\mathbf{F}_\mathbf{k} = \mathbf{F}_{\mathbf{k},\perp} \oplus \mathbf{F}_{\mathbf{k},\mathrm{L}} \oplus \mathbf{F}_{\mathbf{k},\mathrm{T}}$, which correspond to the modes that behave as $e^{i\mathbf{k}\cdot\mathbf{r}}$ within the array plane (with $\mathbf{k}$ being the in-plane wave vector) and are polarized along the complex unit vectors $\tilde{\mathbf{e}}_{\mathbf{k},\perp} = \mathbf{n}$, $\tilde{\mathbf{e}}_{\mathbf{k},\mathrm{L}} = i\mathbf{k}/|\mathbf{k}|$, and $\tilde{\mathbf{e}}_{\mathbf{k},\mathrm{T}} = [\mathbf{n}\times i\mathbf{k}]/|\mathbf{k}|$, with $\mathbf{n}$ being the unit normal to the array plane. The dimension of each of these subspaces is $2N$, with $N = K/3$. Within each subspace, the eigenvectors $\mathbf{F}_{\mathbf{k},l}$, $l = \perp,\mathrm{L},\mathrm{T}$ (with normalization $\langle \mathbf{F}_{\mathbf{k},l}|\mathbf{F}_{\mathbf{k},l}\rangle = 1$) are found to be

$$\mathbf{F}_{\mathbf{k},l} = \frac{1}{\sqrt{2N\omega_{\mathbf{k},l}}}\begin{pmatrix}\frac{1}{\sqrt{m_{\mathrm{eff},l}\omega_{\mathbf{k},l}}}\left[\tilde{\mathbf{e}}_{\mathbf{k},l}e^{i\mathbf{k}\cdot\mathbf{r}_q}\right]_N\\ -i\sqrt{m_{\mathrm{eff},l}\omega_{\mathbf{k},l}}\left[\tilde{\mathbf{e}}_{\mathbf{k},l}e^{i\mathbf{k}\cdot\mathbf{r}_q}\right]_N\end{pmatrix}, \tag{5}$$

with the eigennumbers $\omega_{\mathbf{k},l}$ expressed as

$$\omega_{\mathbf{k},l} = \sqrt{\Omega_l^2 + \frac{e^2 C_{\mathbf{k},l}}{4\pi\varepsilon_0 m_{\mathrm{eff},l}}}, \tag{6}$$

where $C_{\mathbf{k},l} = \sum_{q\neq 0}(\tilde{\mathbf{e}}_{\mathbf{k},l}\cdot\overline{\overline{\Phi}}_{0q}\cdot\tilde{\mathbf{e}}^*_{\mathbf{k},l})\cos(\mathbf{k}\cdot\mathbf{R}_{0q})$ is the interaction factor for the mode of a given polarization [in (6), $\Omega_{\mathrm{L,T}} \equiv \Omega_\parallel$].

Therefore, expanding the (real-valued) state vectors over this basis as $\mathbf{F}(t) = \sum_{l=\perp,\mathrm{L},\mathrm{T}}\sum_{\omega_\mathbf{k}>0}[\alpha_{\mathbf{k},l}(t)\mathbf{F}_{\mathbf{k},l} + \alpha^*_{\mathbf{k},l}(t)\mathbf{F}^*_{\mathbf{k},l}]$ and using the orthogonality of the basis vectors, we express the Hamiltonian (3) as $H = \frac{1}{2}\mathbf{F}^\dagger\mathbf{M}\mathbf{F} = \sum_{l=\perp,\mathrm{L},\mathrm{T}}\sum_{\omega_\mathbf{k}>0}|\alpha_{\mathbf{k},l}|^2$ and obtain from (4) a set of dynamic equations

$$\dot{\alpha}_{\mathbf{k},l} = -i\omega_{\mathbf{k},l}\alpha_{\mathbf{k},l}.$$

It is evident that $\alpha_{\mathbf{k},l}$ has the dimension of the square root of energy. By introducing the real-valued conjugate canonical variables

$$q_{\mathbf{k},l} = \frac{\alpha_{\mathbf{k},l} + \alpha^*_{\mathbf{k},l}}{\omega_{\mathbf{k},l}\sqrt{2}}, \quad \pi_{\mathbf{k},l} = \frac{\alpha_{\mathbf{k},l} - \alpha^*_{\mathbf{k},l}}{i\sqrt{2}}, \tag{7}$$

we reduce the Hamiltonian to the canonical diagonalized form

$$H = \sum_{l=\perp,\mathrm{L},\mathrm{T}}\sum_{\omega_\mathbf{k}>0}\left[\frac{\omega^2_{\mathbf{k},l}q^2_{\mathbf{k},l}}{2} + \frac{\pi^2_{\mathbf{k},l}}{2}\right]. \tag{8}$$

Thus, the dynamics of the system is equivalent to the dynamics of a set of independent harmonic oscillators, each representing a given normal mode of the dynamic system (4).

To quantize the system in the Heisenberg picture we promote the dynamic variables (7) to operators $\hat{q}_{\mathbf{k},l}$ and $\hat{\pi}_{\mathbf{k},l}$ which satisfy the canonical commutation relation $\hat{q}_{\mathbf{k},l}\hat{\pi}_{\mathbf{k},l} - \hat{\pi}_{\mathbf{k},l}\hat{q}_{\mathbf{k},l} = i\hbar$. Introducing the (time-dependent) creation and annihilation operators $\hat{a}^\dagger_{\mathbf{k},l}$, $\hat{a}_{\mathbf{k},l}$, such that

$$\hat{q}_{\mathbf{k},l} = \sqrt{\frac{\hbar}{2\omega_{\mathbf{k},l}}}(\hat{a}^\dagger_{\mathbf{k},l} + \hat{a}_{\mathbf{k},l}), \tag{9}$$

$$\hat{\pi}_{\mathbf{k},l} = i\sqrt{\frac{\hbar\omega_{\mathbf{k},l}}{2}}(\hat{a}^\dagger_{\mathbf{k},l} - \hat{a}_{\mathbf{k},l}), \tag{10}$$

$$\hat{a}_{\mathbf{k},l}\hat{a}^\dagger_{\mathbf{k},l} - \hat{a}^\dagger_{\mathbf{k},l}\hat{a}_{\mathbf{k},l} = 1, \tag{11}$$

we express the total Hamiltonian as

$$\hat{H} = \sum_{l=\perp,\mathrm{L},\mathrm{T}}\sum_{\omega_{\mathbf{k},l}>0}\hbar\omega_{\mathbf{k},l}\left(\hat{a}^\dagger_{\mathbf{k},l}\hat{a}_{\mathbf{k},l} + \frac{1}{2}\right).$$

It is seen that the quantization is equivalent in effect to replacing the classical wave amplitudes by the quantum-mechanical operators as follows: $\alpha_{\mathbf{k},l} \leftrightarrow \sqrt{\hbar\omega_{\mathbf{k},l}}\hat{a}_{\mathbf{k},l}$, $\alpha^*_{\mathbf{k},l} \leftrightarrow \sqrt{\hbar\omega_{\mathbf{k},l}}\hat{a}^\dagger_{\mathbf{k},l}$. Consequently, the state vector is promoted to the following operator:

$$\hat{\mathbf{F}} = \sum_{l=\perp,\mathrm{L},\mathrm{T}}\sum_{\omega_{\mathbf{k},l}>0}\sqrt{\hbar\omega_{\mathbf{k},l}}(\mathbf{F}_{\mathbf{k},l}\hat{a}_{\mathbf{k},l} + \mathbf{F}^*_{\mathbf{k},l}\hat{a}^\dagger_{\mathbf{k},l}). \tag{12}$$

III. POLARITON-TO-POLARITON INTERACTION FOR A PAIR OF MOVING DIELECTRIC SHEETS

Let us consider a pair of identical dielectric sheets separated by distance h (see Fig. 1). The dielectric sheets are modeled as dense planar arrays of electric dipoles, as outlined in the previous section. One of the sheets slides over the other with the relative velocity $\mathbf{v}$ (we consider only the nonrelativistic case in which $v \ll c$). Under our framework, the total Hamiltonian of such a system can be written as

$$H_{\mathrm{tot}} = \tfrac{1}{2}\mathbf{F}_1^\dagger\mathbf{M}\mathbf{F}_1 + \tfrac{1}{2}\mathbf{F}_2^\dagger\mathbf{M}\mathbf{F}_2 + H_{12}, \tag{13}$$

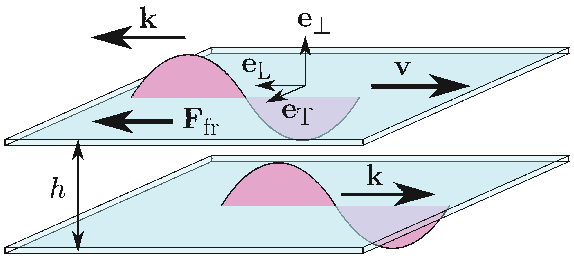

FIG. 1. (Color online) Illustration of the polariton-polariton interaction for two thin dielectric slabs separated by distance h (see Sec. III). The bottom slab is at rest. The upper slab slides with velocity $\mathbf{v}$. The wave vectors of the interacting polaritons in the two slabs are oppositely directed. Generation of such pairs of polaritons (see Sec. IV) results in a friction force $\mathbf{F}_{\rm fr}$ acting on the moving slab (an oppositely directed force of the same magnitude acting on the stationary slab is not shown).

where $\mathbf{F}_{1,2}(t)$ are the state vectors for the two arrays, and H_{12} describes the interaction between the arrays. The interaction term is given by [compare with Eq. (1)]

$$H_{12} = \frac{e^2}{4\pi\varepsilon_0} \sum_{\alpha,\beta=\perp,\mathrm{L,T}} \sum_{s,q} \mathbf{x}_{1,s,\alpha} \cdot \overline{\overline{\Phi}}_{sq}(h) \cdot \mathbf{x}_{2,q,\beta}, \tag{14}$$

where $\overline{\overline{\Phi}}_{sq}(h)$ is defined as in Eq. (2), but with indices s and q running over oscillators in separate arrays, and with $\mathbf{R}_{sq} = \mathbf{r}_{2,q} + \mathbf{v}t - \mathbf{r}_{1,s} + \mathbf{h}$, where $\mathbf{r}_{1,s}$ and $\mathbf{r}_{2,q}$ are the in-plane radius vectors with respect to a fixed oscillator (the "zero" oscillator) in each array, and the vector $\mathbf{h}$ orthogonal to the arrays defines the separation between the two arrays [also note that the term with $s = q$ is now included in the summation (14)].

In Appendix C we derive the quantum-mechanical form of the interaction Hamiltonian (14) for the two arrays in relative motion, and prove that it can be expressed as

$$\hat{H}_{12} = \frac{\hbar}{2} \sum_{\alpha,\beta=\perp,\mathrm{L}} \sum_{\omega_{\mathbf{k}}>0} \frac{g_{\alpha\beta}\sqrt{|\omega_{\mathbf{k},\alpha}^2 - \tilde{\Omega}_\alpha^2||\omega_{\mathbf{k},\beta}^2 - \tilde{\Omega}_\beta^2|}}{\sqrt{\omega_{\mathbf{k},\alpha}\omega_{\mathbf{k},\beta}}} \times (\hat{a}_{1,\mathbf{k},\alpha} + \hat{a}_{1,-\mathbf{k},\alpha}^\dagger)(\hat{a}_{2,\mathbf{k},\beta}^\dagger + \hat{a}_{2,-\mathbf{k},\beta}) e^{-|\mathbf{k}|h} e^{i\mathbf{k}\cdot\mathbf{v}t}, \tag{15}$$

where the tensor $g_{\alpha\beta}$ (such that $|g_{\alpha\beta}| = 1$ when $\alpha = \perp$,L, $\beta = \perp$,L) is defined in Appendix C [Eq. (C7)] and $\tilde{\Omega}_\alpha = \lim_{\mathbf{k}\to 0} \omega_{\mathbf{k},\alpha}$. As is seen from this result, the T-polaritons do not contribute to the interaction Hamiltonian of the two arrays in motion. When deriving Eq. (15) we employ continuous approximation for the arrays, because it is assumed that the array separation h is much greater than the lattice period. In this approximation the interaction between the arrays is equivalent to the interaction between polaritonic modes in a pair of thin dielectric sheets.

Let us note that while this result was obtained assuming that the two dielectric sheets are identical, the representation (15) is general enough to be applicable to a pair of dielectric sheets of different physical nature, as long as the natural modes of the sheets split into the independent polarization states described by the set of eigenvectors introduced in Sec. II. Moreover, Eq. (15) may be generalized to dielectrics with a multiresonant response (i.e., when there are multiple branches of the same polarization type), in which case the indices α and β should run over all interacting branches.

As is evident from (15), the interaction between the slabs can be explained in quantum language as an exchange of polaritons. Indeed, the term $(\hat{a}_{2,\mathbf{k},\beta}^\dagger + \hat{a}_{2,-\mathbf{k},\beta})$ physically corresponds to annihilation of a polariton with the wave vector $-\mathbf{k}$ and creation of a polariton with the wave vector $\mathbf{k}$ in the second slab. At the same time, due to the term $(\hat{a}_{1,\mathbf{k},\alpha} + \hat{a}_{1,-\mathbf{k},\alpha}^\dagger)$, a polariton with the wave vector $-\mathbf{k}$ is created and a polariton with the wave vector $\mathbf{k}$ is annihilated in the first slab.

IV. INDUCED TRANSITIONS BETWEEN POLARITON STATES AND THE FRICTION FORCE

In the previous section we obtained an expression for the total Hamiltonian of a system composed of two thin polarizable slabs sliding one with respect to another with a fixed velocity $\mathbf{v}$. Without any loss of generality, we may assume the first slab is at rest (fixed) and the second one being in motion. Due to a Doppler-like effect, the relative movement gives rise to oscillating terms $e^{i\mathbf{k}\cdot\mathbf{v}t}$ in the interaction Hamiltonian (15). It is known that such a periodic perturbation may induce transitions between the polaritonic states of the slabs.

The well-known Fermi golden rule allows one to calculate the transition rate between an initial state $|i\rangle$ and the final state $|f\rangle$ of a quantum system under a small perturbation $\hat{H}_{\rm pert} = \hat{V}e^{-i\omega t}$ as

$$R_{i\to f} = \frac{2\pi}{\hbar^2}\delta\left(\frac{\mathcal{E}_f - \mathcal{E}_i}{\hbar} - \omega\right)|\langle f|\hat{H}_{\rm pert}|i\rangle|^2, \tag{16}$$

where $\mathcal{E}_i$ and $\mathcal{E}_f$ are the energies in the initial and the final state, respectively. From (16) it is seen that the transition happens only between the states such that $\mathcal{E}_f - \mathcal{E}_i = \hbar\omega$. In our system, the perturbation is due to the interaction between the slabs: $\hat{H}_{\rm pert} = \hat{H}_{12}$.

Let the initial state be the ground state of the system: No polaritons in both slabs, which can be written as $|i\rangle = |0,0\rangle$, and the final state is $|f\rangle = |1_{-\mathbf{k},\alpha}, 1_{\mathbf{k},\beta}\rangle$ (here the first component of the state vector corresponds to the stationary slab and the second component corresponds to the moving slab, thus, $\mathbf{k}$ is the wave vector of a polariton in the moving slab), which means that a pair of oppositely propagating polaritons (in general, with different polarizations denoted by the labels α and β) has been created in the slabs. Evidently, in this case $\mathcal{E}_f - \mathcal{E}_i = \hbar(\omega_{\mathbf{k},\alpha} + \omega_{\mathbf{k},\beta})$. Thus, the frequencies and the wave vectors of the created polaritons (one per slab) satisfy $\mathbf{k}_{1,2}\cdot\mathbf{v} = \pm(\omega_{\mathbf{k},\alpha} + \omega_{\mathbf{k},\beta})$, where $\mathbf{k} \equiv \mathbf{k}_2$.

Calculating $|\langle f|\hat{H}_{12}|i\rangle|^2$ for such a transition that corresponds to a single addend of Eq. (15) we find

$$\begin{aligned} &|\langle 1_{-\mathbf{k},\alpha}, 1_{\mathbf{k},\beta}|\hat{H}_{12}|0,0\rangle|^2 \\ &= \frac{\hbar^2|\omega_{\mathbf{k},\alpha}^2 - \tilde{\Omega}_\alpha^2||\omega_{\mathbf{k},\beta}^2 - \tilde{\Omega}_\beta^2|}{4\omega_{\mathbf{k},\alpha}\omega_{\mathbf{k},\beta}} \\ &\quad\times e^{-2|\mathbf{k}|h}|\langle 1_{-\mathbf{k},\alpha}, 1_{\mathbf{k},\beta}|(\hat{a}_{1,\mathbf{k},\alpha} + \hat{a}_{1,-\mathbf{k},\alpha}^\dagger) \\ &\quad\times(\hat{a}_{2,\mathbf{k},\beta}^\dagger + \hat{a}_{2,-\mathbf{k},\beta})|0_{-\mathbf{k},\alpha}, 0_{\mathbf{k},\beta}\rangle|^2 \\ &= \frac{\hbar^2|\omega_{\mathbf{k},\alpha}^2 - \tilde{\Omega}_\alpha^2||\omega_{\mathbf{k},\beta}^2 - \tilde{\Omega}_\beta^2|}{4\omega_{\mathbf{k},\alpha}\omega_{\mathbf{k},\beta}} e^{-2|\mathbf{k}|h}. \end{aligned} \tag{17}$$

The work of the external forces that is spent onto the creation of the polariton pairs with certain $\mathbf{k}$ and all possible polarizations is, per a time unit,

$$\frac{dW_{\mathbf{k}}^{\text{ext}}}{dt} = \sum_{\alpha,\beta=\perp,\text{L}} \hbar(\omega_{\mathbf{k},\alpha} + \omega_{\mathbf{k},\beta}) R_{i\to f}.$$

This amount of work is numerically equal to the work of the friction force acting on the moving slab (because the work of the oppositely directed force acting on the fixed slab is zero): $W_{\mathbf{k}}^{\text{ext}} = W_{\mathbf{k}}^{\text{fr}}$. Therefore, the pertinent contribution to the friction force is

$$f_{\mathbf{k}} = \frac{dW_{\mathbf{k}}^{\text{fr}}}{v dt} = \sum_{\alpha,\beta=\perp,\text{L}} \frac{\hbar(\omega_{\mathbf{k},\alpha} + \omega_{\mathbf{k},\beta})}{v} R_{i\to f}, \tag{18}$$

where $R_{i\to f}$, from (16) and (17), is

$$R_{i\to f} = \frac{\pi \left|\omega_{\mathbf{k},\alpha}^2 - \tilde{\Omega}_\alpha^2\right| \left|\omega_{\mathbf{k},\beta}^2 - \tilde{\Omega}_\beta^2\right|}{2\omega_{\mathbf{k},\alpha}\omega_{\mathbf{k},\beta}} \times e^{-2|\mathbf{k}|h} \delta(\omega_{\mathbf{k},\alpha} + \omega_{\mathbf{k},\beta} + \mathbf{k}\cdot\mathbf{v}). \tag{19}$$

There is one interesting point about this result that should be mentioned. The expression for $R_{i\to f}$ does not contain the Planck constant, which is an indication that (19) can be derived classically. For example, when only the polaritons of a certain type can be excited in the slabs (for example, with $\alpha = \beta = \text{L}$), the transition rate simplifies to (here for L-type polaritons, $\tilde{\Omega} \equiv \tilde{\Omega}_{\text{L}}$ and $\omega_{\mathbf{k}} \equiv \omega_{\mathbf{k},\text{L}}$)

$$R_{i\to f} = \frac{\pi\left(\omega_{\mathbf{k}}^2 - \tilde{\Omega}^2\right)^2}{2\omega_{\mathbf{k}}^2} e^{-2|\mathbf{k}|h} \delta(2\omega_{\mathbf{k}} + \mathbf{k}\cdot\mathbf{v}). \tag{20}$$

As is shown in Sec. V, a classical analogy of the transition rate (20) can be found from a process of resonant parametric excitation of the electron oscillations at the frequency $\omega_{\mathbf{k}} = |\mathbf{k}\cdot\mathbf{v}|/2$ (previously designated by Pendry as the *washboard effect*[4,8]).

From (18) the total friction force per unit area due to all possible transitions is

$$\begin{aligned}\frac{F_{\text{fr}}}{A} &= \iint \frac{f_{\mathbf{k}}\, d^2\mathbf{k}}{(2\pi)^2} \\ &= \frac{\hbar}{4\pi v} \sum_{\alpha,\beta=\perp,\text{L}} \iint \frac{(\omega_{\mathbf{k},\alpha} + \omega_{\mathbf{k},\beta})\left|\omega_{\mathbf{k},\alpha}^2 - \tilde{\Omega}_\alpha^2\right|\left|\omega_{\mathbf{k},\beta}^2 - \tilde{\Omega}_\beta^2\right|}{2\omega_{\mathbf{k},\alpha}\omega_{\mathbf{k},\beta}} \\ &\quad \times e^{-2|\mathbf{k}|h} \delta(\omega_{\mathbf{k},\alpha} + \omega_{\mathbf{k},\beta} + \mathbf{k}\cdot\mathbf{v})\, d^2\mathbf{k} \\ &= \frac{\hbar}{8\pi v^2} \sum_{\alpha,\beta=\perp,\text{L}} \int \frac{\omega_{\mathbf{k},\alpha} + \omega_{\mathbf{k},\beta}}{\omega_{\mathbf{k},\alpha}\omega_{\mathbf{k},\beta}} \\ &\quad \times \left| \frac{\left(\omega_{\mathbf{k},\alpha}^2 - \tilde{\Omega}_\alpha^2\right)\left(\omega_{\mathbf{k},\beta}^2 - \tilde{\Omega}_\beta^2\right)}{1 + v^{-1}(\partial\omega_{\mathbf{k},\alpha}/\partial k_x + \partial\omega_{\mathbf{k},\beta}/\partial k_x)} \right| e^{-2|\mathbf{k}|h}\, dk_y,\end{aligned} \tag{21}$$

where in the last integral $\mathbf{k} = (k_x, k_y)$, with $k_x = -(\omega_{\mathbf{k},\alpha} + \omega_{\mathbf{k},\beta})/v$, where k_x is the component of the wave vector $\mathbf{k}$ parallel to the velocity.

Note that we have expressed Eq. (21) exclusively in terms of the the dispersion properties of the slab eigenmodes. This suggests that Eq. (21) can be applied not only to the two-dimensional arrays with the modal dispersion given by Eq. (6), but also to systems with qualitatively different dispersion behavior, provided that the polarization waves in these systems are confined within thin layers (e.g., skin depth layers), and split into the same independent polarization states.

For example, we may apply Eq. (21) to thin plasmonic slabs (e.g., slabs of noble metals described by the Drude model) which support short range (SR) and long range (LR) surface plasmon-polariton (SPP) modes.[34] It can be verified that the SR SPP mode of such a slab corresponds to the L-polarized wave of our theory with the parameter $\tilde{\Omega}_{\text{L}} = \lim_{|\mathbf{k}|d\to 0} \omega_{\mathbf{k},\text{SR}} = 0$, where d is the slab thickness. Respectively, the LR SPP mode corresponds to the $\perp$-polarized wave with the parameter $\tilde{\Omega}_\perp = \lim_{|\mathbf{k}|d\to 0} \omega_{\mathbf{k},\text{LR}} = \omega_{\text{p}}$, provided that $|\mathbf{k}| \geqslant \omega_{\text{p}}/c$, where ω_{p} is the plasma frequency of the metal. In addition, for full equivalence it is required that $m_{\text{eff},\perp} = m_{\text{eff},\parallel}$ (see Appendix C).

For such SPP-like modes under the condition $\omega_{\mathbf{k},\text{SR}} \approx \omega_{\mathbf{k},\text{LR}} \approx \omega_{\text{SPP}} = \omega_{\text{p}}/\sqrt{2}$, which holds for strongly confined SPPs with $|\mathbf{k}| \gg \omega_{\text{SPP}}/c$, we obtain for the friction force

$$\frac{F_{\text{fr}}}{A} \approx \frac{\hbar\omega_{\text{SPP}}^3}{\pi v^2} \int e^{-2h\sqrt{(\frac{2\omega_{\text{SPP}}}{v})^2 + k_y^2}}\, dk_y. \tag{22}$$

This result is in agreement with semiclassical theories of quantum friction known from the literature.[4–6] In a more recent work[8] based on a quantum-mechanical model for plasmons on metal surfaces, Pendry obtained a result which differs from (22) (as well as from his original theory[4]) by a factor of 1/2.

Pendry's quantum-mechanical model[8] assumed lossless Drude-type dispersion for the metal conductivity, i.e., it was essentially a free electron plasma model. In contrast, our theory is based on an oscillatory model for the bounded electrons with the characteristic resonant frequency $\omega_0 \neq 0$. This allows us to obtain an important result that does not follow immediately from the quantum-mechanical model of Pendry.

Namely, taking the limit $\omega_0 \to \infty$ under the condition $m_e\omega_0^2 = \text{const}$, which corresponds to arrays of dispersionless oscillators, we find that $\omega_{\mathbf{k},\alpha} \propto \omega_0$ in this limit, and, respectively, $\omega_{\mathbf{k},\alpha}^2 - \tilde{\Omega}_\alpha^2 \propto \omega_0^2$. At the same time, the argument of the exponent in integral (21) is such that $|\mathbf{k}|h \propto \omega_0 h/v \to \infty$. Thus, despite that the factor before the exponent grows as ω_0^3, integral (21) vanishes in this limit at any finite separations $h > 0$ because of the quickly decaying exponential factor in the integrand. Thus, our model predicts (for the nonrelativistic case when $v \ll c$, as the theory is valid only in this case) that the quantum friction vanishes for slabs of nondispersive dielectrics.

This is illustrated numerically in Fig. 2, in which we calculate the friction force per unit area [Eq. (21)] between two identical sheets supporting L-polarized polaritons. In order to make the calculation we take into account the results of Appendix B [Eq. (B4)], from which it follows that $\partial\omega_{\mathbf{k},\alpha}/\partial k_x = [(\omega_{\mathbf{k},\alpha}^2 - \tilde{\Omega}_\alpha^2)/(2\omega_{\mathbf{k},\alpha})][\tilde{C}_{\mathbf{k},\alpha}^{-1}(\partial\tilde{C}_{\mathbf{k},\alpha}/\partial k_x)]$, and in the continuous limit $\tilde{C}_{\mathbf{k},\alpha}^{-1}(\partial\tilde{C}_{\mathbf{k},\alpha}/\partial k_x) = k_x/|\mathbf{k}|$, and substitute these relations into Eq. (21).

In the considered numerical example the polaritonic modes are characterized by $m_{\text{eff,L}}\tilde{\Omega}_{\text{L}}^2 = f \times m_e \times 10^{31}\ \text{s}^{-2} = f \times 9.10938\ \text{kg s}^{-2}$, with the factor f taking the values 0.3, 1, and 3. The sheets are separated by 3 nm and move with the relative velocity $v = 3$ m/s.

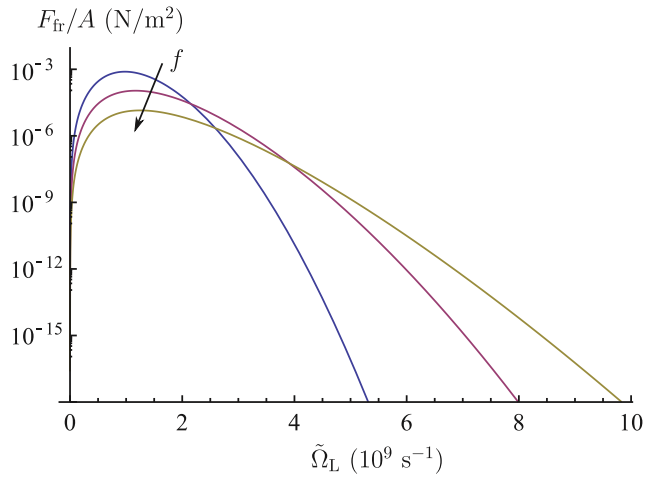

FIG. 2. (Color online) The friction force (per unit area) due to generation of the L-polarized polaritons as a function of the parameter $\tilde{\Omega}_{\rm L}$, under the condition that $m_{\rm eff,L}\tilde{\Omega}_{\rm L}^2 = f \times 9.10938\,{\rm kg\,s^{-2}} = {\rm const}$. The three curves are for the values of f equal to 0.3, 1, and 3. The arrow indicates the direction in which f increases. The two sheets are separated by 3 nm and move with the relative velocity $v = 3$ m/s.

In each of the three curves in Fig. 2 we keep the parameter $m_{\rm eff,L}\tilde{\Omega}_{\rm L}^2$ constant while varying $\tilde{\Omega}_{\rm L}$. One may see that with the increase of $\tilde{\Omega}_{\rm L}$ the friction force initially grows, however, after a certain threshold it decreases monotonically. This confirms that in the limit of no dispersion, the quantum friction vanishes.

In Figs. 3 and 4 we show the dependence of the same friction force on the separation h and the velocity v, respectively. In these calculations, $\tilde{\Omega}_{\rm L} = 10^9$ s^{-1}, while the parameter $m_{\rm eff,L}\tilde{\Omega}_{\rm L}^2$ takes the same values as in Fig. 2. The values of the other parameters are indicated in the figure captions. Note the counterintuitive dependence of the friction force on the velocity: The force initially grows very rapidly with v, however, starting from $v \gtrsim 3$ m/s the friction force monotonically decreases with the velocity. Similar behavior of the friction force can be as well observed in systems involving plasmonic slabs [Eq. (22)].

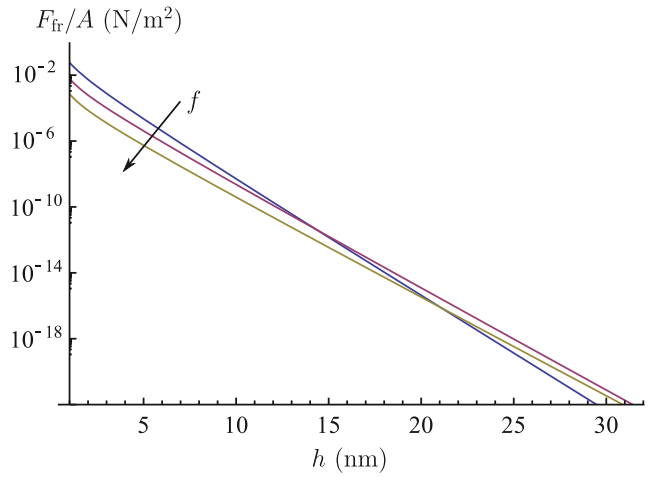

FIG. 3. (Color online) The friction force in the same system as in Fig. 2 as a function of the separation of the sheets, for the case $\tilde{\Omega}_{\rm L} = 10^9$ s^{-2}. The sheets move with the relative velocity $v = 3$ m/s. The meaning of the curves is the same as in Fig. 2.

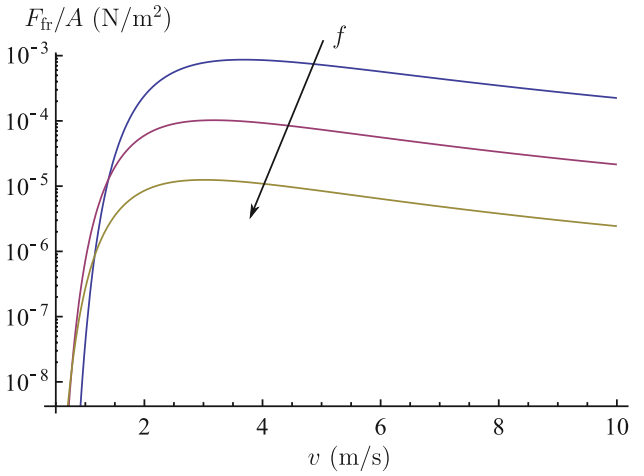

FIG. 4. (Color online) The friction force in the same system as in Fig. 2 as a function of the relative velocity v, for the case $\tilde{\Omega}_{\rm L} = 10^9$ s^{-2}. The slabs are separated by $h = 3$ nm. The meaning of the curves is the same as in Fig. 2.

V. QUANTUM FRICTION FROM A CLASSICAL PERSPECTIVE

In this section we consider a process of parametric excitation of polaritonic oscillations in the two slabs using the classical Hamiltonian formalism. This will allow us to establish a connection between the quantum-mechanical friction force and a classical process, and obtain a classical equivalent of the quantum-mechanical transition rate. To simplify writing, we consider the case when only the polarization waves of a single type are excited in both slabs. Extending the derivation to the case of all polarizations is straightforward.

Let us first derive the dynamic equations for the time-dependent complex amplitudes of the polarization waves in the interacting slabs. It is convenient to switch temporarily to a new orthonormal basis $\mathbf{Q}_{\mathbf{k},l}$, $\mathbf{P}_{\mathbf{k},l}$ in the subspace of the waves of the single polarization we are interested in (for example, with $l = {\rm L}$), such that

$$\mathbf{Q}_{\mathbf{k},l} = \frac{\mathbf{F}_{\mathbf{k},l} + \mathbf{F}^*_{-\mathbf{k},l}}{\sqrt{2}}, \quad \mathbf{P}_{\mathbf{k},l} = i\frac{\mathbf{F}_{\mathbf{k},l} - \mathbf{F}^*_{-\mathbf{k},l}}{\sqrt{2}}, \tag{23}$$

with $\mathbf{F}_{\mathbf{k},l}$ defined by Eq. (5). It is evident that $\mathbf{Q}^\dagger_{\mathbf{k},l}\mathbf{M}\mathbf{Q}_{\mathbf{k},l} = \mathbf{P}^\dagger_{\mathbf{k},l}\mathbf{M}\mathbf{P}_{\mathbf{k},l} = 1$, and $\mathbf{P}^\dagger_{\mathbf{k},l}\mathbf{M}\mathbf{Q}_{\mathbf{k},l} = 0$. In addition, it is seen that $\mathbf{J}\mathbf{M}\mathbf{Q}_{\mathbf{k},l} = -i\omega_{\mathbf{k},l}\mathbf{P}_{\mathbf{k},l}$ and $\mathbf{J}\mathbf{M}\mathbf{P}_{\mathbf{k},l} = i\omega_{\mathbf{k},l}\mathbf{Q}_{\mathbf{k},l}$. In what follows, we suppress the polarization subindex l for brevity.

Expanding the state vectors in the basis of Eq. (23), we write $\mathbf{F}_j(t) = \sum_{\omega_\mathbf{k}>0}(\alpha_{j,\mathbf{k}}\mathbf{F}_\mathbf{k} + \alpha^*_{j,\mathbf{k}}\mathbf{F}^*_\mathbf{k}) = \sum_{\omega_\mathbf{k}>0}(A_{j,\mathbf{k}}\omega_\mathbf{k}\mathbf{Q}_\mathbf{k} + B_{j,\mathbf{k}}\mathbf{P}_\mathbf{k})$, where $A_{j,\mathbf{k}} = (\alpha_{j,\mathbf{k}} + \alpha^*_{j,-\mathbf{k}})/(\omega_\mathbf{k}\sqrt{2})$, $B_{j,\mathbf{k}} = (\alpha_{j,\mathbf{k}} - \alpha^*_{j,-\mathbf{k}})/(i\sqrt{2})$, with $j = 1,2$ labeling the two slabs. Note that $A_{j,-\mathbf{k}} = A^*_{j,+\mathbf{k}}$ and $B_{j,-\mathbf{k}} = B^*_{j,+\mathbf{k}}$.

The dynamic equations for the coupled polarization waves in the two slabs can be formulated (independently of the basis)

within our framework as

$$i\dot{\mathbf{F}}_1(t) = \mathbf{JMF}_1(t) + \mathbf{JM}_{12}\mathbf{F}_2(t), \tag{24}$$

$$i\dot{\mathbf{F}}_2(t) = \mathbf{JMF}_2(t) + \mathbf{JM}_{12}^{\dagger}\mathbf{F}_1(t), \tag{25}$$

where $\mathbf{M}_{12}$ is such that $H_{12} = \mathbf{F}_1^{\dagger}\mathbf{M}_{12}\mathbf{F}_2$. The basis (23) is useful because, as is easy to prove, $\mathbf{M}_{12}\mathbf{P}_{\mathbf{k}} = 0$ and $\mathbf{M}_{12}\mathbf{Q}_{\mathbf{k}} = \frac{e^2}{4\pi\varepsilon_0}\overline{\overline{\mathbf{C}}}_{-\mathbf{k}\,\mathbf{k}}(h)\cdot\mathbf{Q}_{\mathbf{k}}$, where $\overline{\overline{\mathbf{C}}}_{\mathbf{k}_1\mathbf{k}_2}(h)$ is defined in Appendix C by Eq. (C3). Thus, the vectors $\mathbf{Q}_{\mathbf{k}}$ diagonalize the interaction matrix $\mathbf{M}_{12}$ (the vectors $\mathbf{F}_{\mathbf{k}}$ do not have this property).

Deriving from here the dynamic equations for the amplitudes $A_{j,\mathbf{k}}$ and $B_{j,\mathbf{k}}$ and using the aforementioned properties of these quantities and the expression for the interaction dyadic from Sec. III, we find that $\dot{A}_{j,\pm\mathbf{k}} = B_{j,\pm\mathbf{k}}$, $j = 1,2$, and

$$\dot{B}_{1,-\mathbf{k}} = -\omega_{\mathbf{k}}^2 A_{1,-\mathbf{k}} - \left(\omega_{\mathbf{k}}^2 - \tilde{\Omega}^2\right)e^{-|\mathbf{k}|h}e^{+i\mathbf{k}\cdot\mathbf{v}t}A_{2,+\mathbf{k}}^*, \tag{26}$$

$$\dot{B}_{2,+\mathbf{k}}^* = -\omega_{\mathbf{k}}^2 A_{2,+\mathbf{k}}^* - \left(\omega_{\mathbf{k}}^2 - \tilde{\Omega}^2\right)e^{-|\mathbf{k}|h}e^{-i\mathbf{k}\cdot\mathbf{v}t}A_{1,-\mathbf{k}}. \tag{27}$$

From here,

$$\ddot{A}_{1,-\mathbf{k}} = -\omega_{\mathbf{k}}^2 A_{1,-\mathbf{k}} - \left(\omega_{\mathbf{k}}^2 - \tilde{\Omega}^2\right)e^{-|\mathbf{k}|h}e^{+i\mathbf{k}\cdot\mathbf{v}t}A_{2,+\mathbf{k}}^*, \tag{28}$$

$$\ddot{A}_{2,+\mathbf{k}}^* = -\omega_{\mathbf{k}}^2 A_{2,+\mathbf{k}}^* - \left(\omega_{\mathbf{k}}^2 - \tilde{\Omega}^2\right)e^{-|\mathbf{k}|h}e^{-i\mathbf{k}\cdot\mathbf{v}t}A_{1,-\mathbf{k}}. \tag{29}$$

These two equations are the dynamic equations that we need. We have written these equations in a form that highlights the coupling between oppositely propagating polarization waves. As one can see, Eqs. (28) and (29) are ordinary linear differential equations with a time-dependent coupling parameter. On the other hand, it is seen that these equations correspond to a system of two coupled oscillators, in which the alternating coupling strength plays a role of a parametric pump. Thus, for the system of two moving slabs these equations constitute the mathematical formulation of *the washboard effect* mentioned in Pendry's works.[4,8] Analogous equations appear, for example, in the theory of parametric amplifiers.[28–30]

In order to solve Eqs. (28) and (29) we make a substitution

$$A_{1,-\mathbf{k}}(t) = u_1(t)e^{+i\frac{\mathbf{k}\cdot\mathbf{v}}{2}t}, \quad A_{2,+\mathbf{k}}^*(t) = u_2(t)e^{-i\frac{\mathbf{k}\cdot\mathbf{v}}{2}t},$$

after which we obtain

$$\ddot{u}_1 + i(\mathbf{k}\cdot\mathbf{v})\dot{u}_1 - \frac{(\mathbf{k}\cdot\mathbf{v})^2}{4}u_1 = -\omega_{\mathbf{k}}^2 u_1 - \left(\omega_{\mathbf{k}}^2 - \tilde{\Omega}^2\right)e^{-|\mathbf{k}|h}u_2, \tag{30}$$

$$\ddot{u}_2 - i(\mathbf{k}\cdot\mathbf{v})\dot{u}_2 - \frac{(\mathbf{k}\cdot\mathbf{v})^2}{4}u_2 = -\omega_{\mathbf{k}}^2 u_2 - \left(\omega_{\mathbf{k}}^2 - \tilde{\Omega}^2\right)e^{-|\mathbf{k}|h}u_1, \tag{31}$$

which is a system of two ordinary linear differential equations with constant parameters. Therefore, we may look for the solution of (30) and (31) having the form $u_j(t) = c_j e^{\lambda_{\mathbf{k}}t}$, which results in the following characteristic equation for $\lambda_{\mathbf{k}}$:

$$\left[\lambda_{\mathbf{k}}^2 + \omega_{\mathbf{k}}^2 - \frac{(\mathbf{k}\cdot\mathbf{v})^2}{4}\right]^2 + (\mathbf{k}\cdot\mathbf{v})^2\lambda_{\mathbf{k}}^2 - \left(\omega_{\mathbf{k}}^2 - \tilde{\Omega}^2\right)^2 e^{-2|\mathbf{k}|h} = 0.$$

This biquadratic equation can be easily solved. The result is

$$\lambda_{\mathbf{k}}^2 = -\omega_{\mathbf{k}}^2 - \frac{(\mathbf{k}\cdot\mathbf{v})^2}{4} \pm \sqrt{\omega_{\mathbf{k}}^2(\mathbf{k}\cdot\mathbf{v})^2 + \left(\omega_{\mathbf{k}}^2 - \tilde{\Omega}^2\right)^2 e^{-2|\mathbf{k}|h}}. \tag{32}$$

Under the assumption of weak coupling (which is essentially the same as the small perturbation assumption in the quantum theory) we may approximate the square root in (32) and write

$$\begin{aligned}\lambda_{\mathbf{k}}^2 &\approx -\omega_{\mathbf{k}}^2 - \frac{(\mathbf{k}\cdot\mathbf{v})^2}{4} \pm \omega_{\mathbf{k}}|\mathbf{k}\cdot\mathbf{v}|\left[1 + \frac{\left(\omega_{\mathbf{k}}^2 - \tilde{\Omega}^2\right)^2 e^{-2|\mathbf{k}|h}}{2\omega_{\mathbf{k}}^2(\mathbf{k}\cdot\mathbf{v})^2}\right] \\ &= -\left(\omega_{\mathbf{k}} \mp \frac{|\mathbf{k}\cdot\mathbf{v}|}{2}\right)^2 \pm \frac{\left(\omega_{\mathbf{k}}^2 - \tilde{\Omega}^2\right)^2 e^{-2|\mathbf{k}|h}}{2\omega_{\mathbf{k}}|\mathbf{k}\cdot\mathbf{v}|}.\end{aligned} \tag{33}$$

The case of resonant parametric amplification occurs with the choice of upper signs in (33) because in this case, for the polarization waves with the wave vectors such that

$$\left|\omega_{\mathbf{k}} - \frac{|\mathbf{k}\cdot\mathbf{v}|}{2}\right| < \frac{\left|\omega_{\mathbf{k}}^2 - \tilde{\Omega}^2\right|e^{-|\mathbf{k}|h}}{\sqrt{2\omega_{\mathbf{k}}|\mathbf{k}\cdot\mathbf{v}|}}, \tag{34}$$

there exists a real root of (33) satisfying $\lambda_{\mathbf{k}} > 0$. The amplitude of such waves grows exponentially with time.

The maximum amplification occurs for the polarization waves which are in exact resonance with the parametric pump, i.e., when $\omega_{\mathbf{k}} = |\mathbf{k}\cdot\mathbf{v}|/2$. For these waves, $\lambda_{\mathbf{k}} = \lambda_{0,\mathbf{k}} > 0$, where

$$\lambda_{0,\mathbf{k}} = \frac{\left|\omega_{\mathbf{k}}^2 - \tilde{\Omega}^2\right|e^{-|\mathbf{k}|h}}{2\omega_{\mathbf{k}}}. \tag{35}$$

Note that such a growing solution is always accompanied by a decaying one which has $\lambda_{\mathbf{k}} = -\lambda_{0,\mathbf{k}} < 0$.

For the polarization waves which are not in exact resonance but still satisfy the condition (34), the amplification rate $\lambda_{\mathbf{k}} > 0$ can be approximated as

$$\lambda_{\mathbf{k}} \approx \sqrt{\lambda_{0,\mathbf{k}}^2 - \left(\omega_{\mathbf{k}} - \frac{|\mathbf{k}\cdot\mathbf{v}|}{2}\right)^2} \leqslant \lambda_{0,\mathbf{k}} \tag{36}$$

because within the narrow range (34) it is possible to replace $|\mathbf{k}\cdot\mathbf{v}|$ by $2\omega_{\mathbf{k}}$ in the second parcel of the last identity of Eq. (33).

To further understand the structure of the exponentially growing solutions we substitute $u_j = c_{j,\mathbf{k}}^* e^{\lambda_{\mathbf{k}}t}$ [with $\lambda_{\mathbf{k}}$ given by (36)] into the linear system (30) and (31), keeping in the result only the terms up to the first order with respect to the small parameter $\lambda_{0,\mathbf{k}}$. In this way we find that for such waves $c_{2,\mathbf{k}}/c_{1,\mathbf{k}} = e^{i\psi}$, being $\psi = \arcsin[\mathrm{sgn}(\omega_{\mathbf{k}}^2 - \tilde{\Omega}^2)] + \arccos[\mathrm{sgn}(\mathbf{k}\cdot\mathbf{v})(\lambda_{\mathbf{k}}/\lambda_{0,\mathbf{k}})]$, i.e., the polarization waves parametrically excited in the two slabs have the same intensity, but, in general, different initial phase.

On the other hand, for these waves $A_{1,\mathbf{k}} = c_{1,\mathbf{k}}e^{(\lambda_{\mathbf{k}} - i\frac{\mathbf{k}\cdot\mathbf{v}}{2})t}$ and $A_{2,\mathbf{k}} = c_{2,\mathbf{k}}e^{(\lambda_{\mathbf{k}} + i\frac{\mathbf{k}\cdot\mathbf{v}}{2})t}$, while $|A_{1,\mathbf{k}}| = |A_{2,\mathbf{k}}|$. Returning back to the original basis $\mathbf{F}_{\mathbf{k}} = (\mathbf{Q}_{\mathbf{k}} - i\mathbf{P}_{\mathbf{k}})/\sqrt{2}$ we may write for the polarization waves within the amplification range:

$$\mathbf{F}_j(t) = \sum_{\mathbf{k}_{\mathrm{ampl}}}[\alpha_{j,\mathbf{k}}(t)\mathbf{F}_{\mathbf{k}} + \alpha_{j,\mathbf{k}}^*(t)\mathbf{F}_{\mathbf{k}}^*], \tag{37}$$

where we sum over the wave vectors that satisfy Eq. (34) and consider only the growing solutions with $\lambda_{\mathbf{k}} > 0$. The

amplitudes $\alpha_{j,\mathbf{k}} = (\omega_{\mathbf{k}} A_{j,\mathbf{k}} + i\dot{A}_{j,\mathbf{k}})/\sqrt{2}$ satisfy

$$\alpha_{1,\mathbf{k}}(t) = \frac{1}{\sqrt{2}}\left(\omega_{\mathbf{k}} + \frac{\mathbf{k}\cdot\mathbf{v}}{2} + i\lambda_{\mathbf{k}}\right)A_{1,\mathbf{k}}(t), \tag{38}$$

$$\alpha_{2,\mathbf{k}}(t) = \frac{1}{\sqrt{2}}\left(\omega_{\mathbf{k}} - \frac{\mathbf{k}\cdot\mathbf{v}}{2} + i\lambda_{\mathbf{k}}\right)A_{2,\mathbf{k}}(t). \tag{39}$$

The eigenvectors $\mathbf{F}_{\mathbf{k}}$ behave as $e^{i\mathbf{k}\cdot\mathbf{r}}$ in the slab plane, therefore, the complex modes in the sum (37) have the propagation factor $e^{\pm i\mathbf{k}\cdot(\mathbf{r}_1 - \frac{\mathbf{v}t}{2})}$ in the first slab, while the same modes in the second slab behave as $e^{\pm i\mathbf{k}\cdot(\mathbf{r}_2 + \frac{\mathbf{v}t}{2})}$, i.e., the polarization waves generated in the first slab *all* propagate with the velocity $\mathbf{v}/2$ with respect to the local coordinate frame fixed in this slab, while the same waves in the second slab propagate in the opposite direction (with the velocity $-\mathbf{v}/2$) with respect to the local frame.

Additionally, it follows from Eqs. (38) and (39), and the fact that $A_{j,-\mathbf{k}} = A^*_{j,+\mathbf{k}}$, that $|\alpha_{1,+\mathbf{k}}| \ll |\alpha_{1,-\mathbf{k}}|$ and $|\alpha_{2,-\mathbf{k}}| \ll |\alpha_{2,+\mathbf{k}}|$, where $\mathbf{k}$ is such that $\mathbf{k}\cdot\mathbf{v} < 0$, because within the amplification range $\lambda_{\mathbf{k}} \ll \omega_{\mathbf{k}}$ and $\omega_{\mathbf{k}} \approx |\mathbf{k}\cdot\mathbf{v}|/2$. Taking into account these results, we may express the total energy $\mathcal{E} = H_{\text{tot}}$ [Eq. (13)] of the polarization waves generated in both slabs (neglecting the small interaction term) as

$$\mathcal{E} \approx \sum_{\mathbf{k}_{\text{ampl}}}(|\alpha_{1,\mathbf{k}}|^2 + |\alpha_{2,\mathbf{k}}|^2) \approx \sum_{\substack{\mathbf{k}\cdot\mathbf{v}<0\\(\text{ampl})}} \mathcal{E}_{\mathbf{k}}(t_0)e^{2\lambda_{\mathbf{k}}(t-t_0)}, \tag{40}$$

where $\mathcal{E}_{\mathbf{k}}(t_0) = |\alpha_{1,-\mathbf{k}}(t_0)|^2 + |\alpha_{2,+\mathbf{k}}(t_0)|^2 = 2|\alpha_{1,-\mathbf{k}}(t_0)|^2$ is the contribution to the polaritonic energy (at the time instant $t = t_0$) of a pair of dominantly excited eigenmodes of the two slabs characterized with oppositely directed wave vectors.

In order to establish a correspondence between the quantum-mechanical polariton generation problem and the classical parametric excitation problem we note that the approach of Sec. IV assumes that the polaritons generated in the transitions $|0,0\rangle \to |1_{-\mathbf{k}},1_{\mathbf{k}}\rangle$ get absorbed (or in any other way leave the system) soon after being generated. This ensures that all subsequent transitions initiate from the ground state, which allows us to express the quantum friction only in terms of such transitions. Thus, we may say that in the processes we are interested in, the rate at which the polaritons are generated is equilibrated by the absorption rate of the same polaritons.

In what follows we consider the classical parametric generation problem under a similar assumption that, in steady state, the rate of pumping the energy into the system is compensated by some concurrent absorption process. We do not need to specify any details about this process except that we assume that there is a dynamic equilibrium between the two concurrent processes, and that for the real polaritonic state characterized with a certain $\mathbf{k}$ that belongs to the amplification range (34) such an equilibrium is reached at a certain energy level $\mathcal{E}_{\mathbf{k}} > 0$, which is a smooth function of $\mathbf{k}$. It is evident that in steady state only the polaritonic solutions with $\lambda_{\mathbf{k}} > 0$ may contribute to this dynamic equilibrium.

One may picture such a steady state as follows. Consider that at a time instant t_0 the total polaritonic energy $\mathcal{E}$ was at the equilibrium level $\mathcal{E}_0$. After a small time interval dt, due to the parametric amplification process, the polaritonic energy may grow by a small amount $d\mathcal{E}$ up to $\mathcal{E}_0 + d\mathcal{E}$. The action of the absorbing process is such that during this small interval of time it absorbs exactly the same amount of energy as it was generated, i.e., the same $d\mathcal{E}$. The dynamics of the parametric amplification allows us to calculate $d\mathcal{E}/dt$. Indeed, if there were no absorption, the energy of polarization waves within the amplification range would grow as given by Eq. (40). Differentiating (40) with respect to time we obtain for the total energy growth rate at $t = t_0$:

$$\frac{d\mathcal{E}}{dt} = \sum_{\substack{\mathbf{k}\cdot\mathbf{v}<0\\(\text{ampl})}} 2\lambda_{\mathbf{k}}\mathcal{E}_{\mathbf{k}}. \tag{41}$$

Using (36) we express (41) as

$$\begin{aligned}\frac{d\mathcal{E}}{dt} &= 2\sum_{\substack{\mathbf{k}\cdot\mathbf{v}<0\\(\text{ampl})}} \mathcal{E}_{\mathbf{k}}\lambda_{0,\mathbf{k}}\sqrt{1 - \frac{(\omega_{\mathbf{k}} - |\mathbf{k}\cdot\mathbf{v}|/2)^2}{\lambda_{0,\mathbf{k}}^2}}\\ &= \frac{2A}{(2\pi)^2}\iint_{\substack{\mathbf{k}\cdot\mathbf{v}<0\\(\text{ampl})}} \mathcal{E}_{\mathbf{k}}\lambda_{0,\mathbf{k}}\sqrt{1 - \frac{(\omega_{\mathbf{k}} + k_x v/2)^2}{\lambda_{0,\mathbf{k}}^2}}\,dk_x\,dk_y,\end{aligned} \tag{42}$$

where we replaced summation over discrete states by integration over the wave vectors $\mathbf{k} = (k_x, k_y)$ in the slab plane, with the k_x component antiparallel to the velocity and $A \to \infty$ being the broadside area of the slabs.

At a fixed k_y the inner integration in (42) is done over a small interval of the width

$$\Delta k_x \approx \frac{2\lambda_{0,\mathbf{k}}}{|\partial\omega_{\mathbf{k}}/\partial k_x + v/2|}.$$

Within this small interval we may approximate $\lambda_{0,\mathbf{k}}$ by its value at the middle point of the interval, so that it becomes independent of k_x. The same approximation can be used for the polaritonic energy $\mathcal{E}_{\mathbf{k}}$. Then, introducing a new variable $\kappa = \lambda_{0,\mathbf{k}}^{-1}(\omega_{\mathbf{k}} + k_x v/2)$, we obtain

$$\begin{aligned}\frac{d\mathcal{E}}{dt} &= \frac{2A}{(2\pi)^2}\int \frac{\mathcal{E}_{\mathbf{k}}\lambda_{0,\mathbf{k}}^2\,dk_y}{|\partial\omega_{\mathbf{k}}/\partial k_x + v/2|}\int_{-1}^{1}\sqrt{1-\kappa^2}\,d\kappa\\ &= \frac{2A}{(2\pi)^2}\int \frac{\mathcal{E}_{\mathbf{k}}\lambda_{0,\mathbf{k}}^2\,dk_y}{|\partial\omega_{\mathbf{k}}/\partial k_x + v/2|}\frac{\pi}{2},\end{aligned} \tag{43}$$

which is the same as

$$\frac{d\mathcal{E}}{dt} = \frac{A}{(2\pi)^2}\iint 2\pi\lambda_{0,\mathbf{k}}^2\mathcal{E}_{\mathbf{k}}\delta(2\omega_{\mathbf{k}} + \mathbf{k}\cdot\mathbf{v})\,d^2\mathbf{k}.$$

The increase in the polaritonic energy is due to the mechanical work done on the moving slab: $d\mathcal{E}/dt = vF_{\text{class}}$, therefore, we may write for the force acting on this slab (per unit area)

$$\frac{F_{\text{class}}}{A} = \frac{1}{v(2\pi)^2}\iint 2\pi\lambda_{0,\mathbf{k}}^2\mathcal{E}_{\mathbf{k}}\delta(2\omega_{\mathbf{k}} + \mathbf{k}\cdot\mathbf{v})\,d^2\mathbf{k}, \tag{44}$$

which is the classical analogy of the quantum friction force. Substituting here the expression for $\lambda_{0,\mathbf{k}}$ from Eq. (35) and comparing Eqs. (44) and (20) we immediately obtain that

$$\frac{F_{\text{class}}}{A} = \frac{1}{v(2\pi)^2}\iint R_{\text{gen}}\mathcal{E}_{\mathbf{k}}\,d^2\mathbf{k}, \tag{45}$$

with the classical equivalent of the polariton generation rate R_{gen}, which is identical to the quantum-mechanical transition rate from Eq. (20):

$$R_{\text{gen}} = 2\pi\lambda_{0,\mathbf{k}}^2\delta(2\omega_{\mathbf{k}} + \mathbf{k}\cdot\mathbf{v}) = R_{i\to f}. \tag{46}$$

The quantum result for the friction force due to the transitions *from the ground state* is recovered from (45) by replacing $\mathcal{E}_{\mathbf{k}}$ by $2\hbar\omega_{\mathbf{k}}$, which is the zero-point energy of *four* modes with the wave vectors $\pm\mathbf{k}$ in both slabs. Note, however, that one might as well argue that only *two* modes (the mode with $\mathbf{k}\cdot\mathbf{v} > 0$ in the first slab, and the mode with $\mathbf{k}\cdot\mathbf{v} < 0$ in the second slab) should be considered, as these are the modes most relevant in the classical problem [see the discussion above Eq. (40)], in which case one would have $\mathcal{E}_{\mathbf{k}} = 2 \times (\hbar\omega_{\mathbf{k}}/2) = \hbar\omega_{\mathbf{k}}$.

There is, in fact, no contradiction here, because the correspondence principle requires that the two approaches (the classical one and the quantum one) match only when the initial number of quanta in the system is large. From Eq. (40) it is evident that such a correspondence is, indeed, in place: The quantization of the polarization waves in both slabs is equivalent to replacing $|\alpha_{j,\mathbf{k}}|^2$ with $\hbar\omega_{\mathbf{k}}(n_{\mathbf{k}} + 1/2)$, where $n_{\mathbf{k}}$ is the number of quanta, therefore, $\mathcal{E}_{\mathbf{k}} = 2|\alpha_{1,-\mathbf{k}}|^2 \approx 2\hbar\omega_{\mathbf{k}}n_{\mathbf{k}}$, when $n_{\mathbf{k}} \gg 1$. The same result can be obtained by considering quantum transitions initiating from a state with a *large* number of quanta, instead of the ground state.

VI. CONCLUSION

In this work we have considered the quantum friction force resulting from generation of polariton pairs in thin moving dielectric slabs (modeled as two-dimensional arrays of dipoles) separated by a vacuum gap. Using a harmonic oscillator model for the polarizable atoms of the dielectric we have proven that the quantum friction completely vanishes in nondispersive dielectrics at nonrelativistic velocities $v \ll c$.

When the dispersion is present, the quantum friction resulting from generation of polaritons in moving dielectric slabs appears somewhat similar to the Cherenkov or Smith-Purcell effects, in which charges moving with a velocity above a certain threshold start losing their kinetic energy due to a generation of photons.

In the quantum friction phenomenon, however, the dielectric slabs are electrically neutral and, thus, a better physical model is required. In order to find such a model, in this work we have established a link between generation of quasiparticles in moving slabs by quantum transitions and the classical process of parametric amplification of the field fluctuations in the same slabs.

The theory of Sec. V shows that even in a classical picture the movement of one slab over the other may result in the amplification of the classical electromagnetic field, resulting from the transfer of kinetic energy of the moving slab to the radiation field. The same result also demonstrates how the quasiparticle generation rate which is usually calculated from the Fermi golden rule can be obtained by solving a related classical parametric amplification problem.

APPENDIX A: HAMILTONIAN DYNAMICS OF ELECTRON OSCILLATIONS IN A DIELECTRIC SLAB

We are interested in collective oscillations of the bounded electrons in a dielectric slab. Because the bounded electrons belong to atoms which are electrically neutral as a whole, the oscillations of these electrons appear (to the first degree of approximation) as electric dipole harmonic oscillations with the effective dipole moments $\mathbf{d} = e\mathbf{x}$, where $\mathbf{x}$ is the electron displacement. For simplicity we assume a cubic lattice and isotropic dipole oscillators (anisotropy, however, will reappear in the model at a later step).

For such an ensemble of interacting dipole oscillators, the total Hamiltonian can be written as

$$H = H_0 + H_{\text{int}}, \tag{A1}$$

where H_0 is

$$H_0 = \sum_m \left(\frac{m_e\omega_0^2\mathbf{x}_m^2}{2} + \frac{\mathbf{p}_m^2}{2m_e} \right) \tag{A2}$$

and the interaction Hamiltonian is, neglecting all retardation effects,

$$H_{\text{int}} = \frac{e^2}{8\pi\varepsilon_0} \sum_{\substack{m,n \\ m\neq n}} \frac{\mathbf{x}_m\cdot\mathbf{x}_n - 3(\mathbf{u}_{mn}\cdot\mathbf{x}_m)(\mathbf{u}_{mn}\cdot\mathbf{x}_n)}{R_{mn}^3}, \tag{A3}$$

where $\mathbf{R}_{mn} = \mathbf{u}_{mn}R_{mn}$ is the radius vector from the mth oscillator to the nth one, and the indices m and n run over all oscillators in the slab.

Such a form of the Hamiltonian corresponds to the single-electron dynamic equation of the form

$$m_e\ddot{\mathbf{x}}_m + m_e\omega_0^2\mathbf{x}_m = e\mathbf{E}_m^{\text{loc}}, \tag{A4}$$

where $\mathbf{x}_m$ is the displacement of the mth electron, $e = -|e|$ is the electron charge, m_e is the electron mass ($m_e \ll m_{\text{atom}}$), ω_0 is the characteristic frequency of the oscillations, and the local field $\mathbf{E}_m^{\text{loc}}$ is produced by all other dipoles except $\mathbf{d}_m$:

$$\mathbf{E}_m^{\text{loc}} = -\frac{1}{4\pi\varepsilon_0} \sum_{n\neq m} \frac{\mathbf{d}_n - 3\mathbf{u}_{mn}(\mathbf{u}_{mn}\cdot\mathbf{d}_n)}{R_{mn}^3}.$$

Let us divide the dielectric slab into macroscopic cubic cells with the dimensions equal to the slab thickness. Each cell contains a large number of polarized atoms, which we model as electric dipole oscillators. Because we are interested only in the dominant modes propagating along the slab under the condition that the slab thickness is much less than the wavelength, we may assume that the dipoles within a single cell are all (on average) polarized along the same direction and oscillate in-phase. The amplitude profile of these oscillations within a single cell is approximately uniform in the plane of the slab, while in the orthogonal direction it is symmetric (even) with respect to the middle plane of the slab.

Physically, the above assumptions mean that the dipole oscillators within a single cell are strongly coupled. The cell symmetry suggests that the collective dynamics of these oscillators can be described with just a pair of conjugate-canonical vector variables $\mathbf{x}_{s,l}$ and $\mathbf{p}_{s,l}$ per cell (indexed by s) per polarization type (indexed by $l = \parallel, \perp$). The latter takes into account that the interaction energy in the modes polarized across the slab ($\perp$-polarized modes) and along the slab ($\parallel$-polarized modes) can be different, as is evident from the form of the interaction Hamiltonian (A3).

It is straightforward to prove that these variables can be defined by the following relations (here the index m runs over

the oscillators belonging to the same cell):

$$\mathbf{x}_m = f_{m,\parallel}\mathbf{x}_{s,\parallel} + f_{m,\perp}\mathbf{x}_{s,\perp}, \tag{A5}$$

$$\mathbf{p}_m = \left(\frac{m_e}{m_{\mathrm{eff},\parallel}}\right) f_{m,\parallel}\mathbf{p}_{s,\parallel} + \left(\frac{m_e}{m_{\mathrm{eff},\perp}}\right) f_{m,\perp}\mathbf{p}_{s,\perp}, \tag{A6}$$

where the amplitude coefficients $f_{m,l}$ (such that $\sum_m f_m = 1$) determine the profile of the respective modes, and $\dot{\mathbf{x}}_{s,l} = \mathbf{p}_{s,l}/m_{\mathrm{eff},l}$.

Under these assumptions, the total Hamiltonian of an isolated cell (which includes the interaction between the oscillators in the same cell) can be written as

$$H_{0,s} = \sum_{l=\parallel,\perp}\left(\frac{m_{\mathrm{eff},l}\Omega_l^2}{2}\mathbf{x}_{s,l}^2 + \frac{\mathbf{p}_{s,l}^2}{2m_{\mathrm{eff},l}}\right), \tag{A7}$$

with the effective parameters

$$\Omega_l^2 = \omega_0^2 + \frac{e^2}{4\pi\varepsilon_0 m_e}\frac{\sum_m\sum_{n\neq m} f_{m,l}f_{n,l}\Phi_{mn,l}}{\sum_m f_m^2}, \tag{A8}$$

$$m_{\mathrm{eff},l} = m_e\sum_m f_{m,l}^2, \tag{A9}$$

where the indices m and n iterate over the oscillators in the cell, and $\Phi_{mn,l} = (1-3\cos^2\alpha_{mn,l})/R_{mn}^3$, where $\cos\alpha_{mn,l} = (\mathbf{u}_{mn}\cdot\mathbf{x}_{s,l})/|\mathbf{x}_{s,l}|$, $l = \parallel,\perp$. The cross-term corresponding to the interaction between the $\parallel$- and $\perp$-polarized dipoles within a single cell vanishes from (A7) due to the assumed symmetry of the polarization distribution in a cubic cell (see above).

On the other hand, the coupling between two separate cells is described by the interaction Hamiltonian

$$H_{\mathrm{int},sq} = \frac{e^2}{4\pi\varepsilon_0}\sum_{m,n}\sum_{l,l'=\parallel,\perp} f_{m,l}f_{n,l'} \times \frac{\mathbf{x}_{s,l}\cdot\mathbf{x}_{q,l'} - 3(\mathbf{u}_{mn}\cdot\mathbf{x}_{s,l})(\mathbf{u}_{mn}\cdot\mathbf{x}_{q,l'})}{R_{mn}^3}, \tag{A10}$$

where the indices m and n run over oscillators in two distinct cells (indexed by s and q, $s\neq q$).

We may approximate the radius-vector $\mathbf{R}_{mn} = \mathbf{u}_{mn}R_{mn}$ in Eq. (A10) by the radius-vector between the middle points of the two cells: $\mathbf{u}_{mn}R_{mn} \approx \mathbf{u}_{sq}R_{sq}$ (which is the same as concentrating the dipole moments at the middle points of the cells). Under this approximation, taking into account that $\sum_{mn} f_{m,l}f_{n,l'} = 1$, we obtain from Eqs. (A7) and (A10) the total Hamiltonian of Sec. II [Eq. (1)].

APPENDIX B: SPECTRUM OF THE OPERATOR JM AND ITS PROPERTIES

As is seen from Eq. (4), the dispersion equation for the normal modes on a single array is $\mathbf{JMF}_\mathbf{k} = \omega_\mathbf{k}\mathbf{F}_\mathbf{k}$, with $\mathbf{M}$ being the matrix of the quadratic form $H = \frac{1}{2}\mathbf{F}^\dagger\mathbf{MF}$ consistent with Eq. (1). It is evident that in an infinite regular array the normal modes are harmonic waves, and, thus, in such a mode, $\mathbf{x}_q, \mathbf{p}_q \propto e^{i\mathbf{k}\cdot\mathbf{r}_q}$, where $\mathbf{k}$ is the in-plane wave vector of a mode. Therefore,

$$\mathbf{F}_\mathbf{k} = \begin{pmatrix}[\mathbf{x}_\mathbf{k}e^{i\mathbf{k}\cdot\mathbf{r}_q}]_N \\ [\mathbf{p}_\mathbf{k}e^{i\mathbf{k}\cdot\mathbf{r}_q}]_N\end{pmatrix}, \tag{B1}$$

with N being the number of oscillators in the array: $N = K/3$.

Based on Eqs. (1) and (B1) it is simple to prove that the dispersion equation reduces to

$$\left[m_{\mathrm{eff},\parallel}(\omega_\mathbf{k}^2 - \Omega_\parallel^2)\bar{\bar{\mathbf{I}}}_\parallel + m_{\mathrm{eff},\perp}(\omega_\mathbf{k}^2 - \Omega_\perp^2)\bar{\bar{\mathbf{I}}}_\perp - \frac{e^2}{4\pi\varepsilon_0}\bar{\bar{\mathbf{C}}}_\mathbf{k}\right]\cdot\mathbf{x}_\mathbf{k} = 0, \tag{B2}$$

where $\bar{\bar{\mathbf{C}}}_\mathbf{k}$ is the interaction dyadic defined by

$$\bar{\bar{\mathbf{C}}}_\mathbf{k} = \sum_{q\neq 0}\bar{\bar{\Phi}}_{0q}e^{i\mathbf{k}\cdot\mathbf{R}_{0q}} = \sum_{q\neq 0}\bar{\bar{\Phi}}_{0q}\cos(\mathbf{k}\cdot\mathbf{R}_{0q}).$$

It is clear from Eqs. (1) and (2) that the total Hamiltonian $H = H_0 + H_{\mathrm{int}}$ splits into two independent addends: $H = H_\perp(\mathbf{p}_{s,\perp},\mathbf{x}_{s,\perp}) + H_\parallel(\mathbf{p}_{s,\parallel},\mathbf{x}_{s,\parallel})$. Hence, the in-plane and the out-of-plane oscillations are completely uncoupled. Moreover, it can be verified that in isotropic (e.g., square or hexagonal) dense lattices the interaction between the in-plane modes polarized along $\mathbf{k}$ (longitudinal $\parallel$ modes) and perpendicular to $\mathbf{k}$ (transverse $\parallel$ modes) is negligible (more strictly, in an isotropic array such interaction vanishes for $\mathbf{k}$ directed along the primitive lattice vectors, while in the continuous medium limit it vanishes for arbitrary directed $\mathbf{k}$). Hence, within the continuous limit approximation, the unit vectors $\mathbf{e}_{\mathbf{k},l}$ given by $\mathbf{e}_{\mathbf{k},\perp} = \mathbf{n}$, $\mathbf{e}_{\mathbf{k},\mathrm{L}} = \mathbf{k}/|\mathbf{k}|$, and $\mathbf{e}_{\mathbf{k},\mathrm{T}} = [\mathbf{n}\times\mathbf{k}]/|\mathbf{k}|$, where $\mathbf{n}$ is the unit normal to the array plane, diagonalize the interaction dyadic $\bar{\bar{\mathbf{C}}}_\mathbf{k}$, and thus also the complete tensor in Eq. (B2). Therefore, within this approximation the phase vector space can be divided into three independent subspaces: $\mathbf{F}_\mathbf{k} = \mathbf{F}_{\mathbf{k},\perp}\oplus\mathbf{F}_{\mathbf{k},\mathrm{L}}\oplus\mathbf{F}_{\mathbf{k},\mathrm{T}}$. The dimension of each of these subspaces is $2N$. The frequency dispersion of each normal mode can be computed from $m_{\mathrm{eff},l}(\omega_\mathbf{k}^2 - \Omega_l^2) - \frac{e^2}{4\pi\varepsilon_0}C_{\mathbf{k},l} = 0$, $l = \perp,\mathrm{L},\mathrm{T}$ (with $m_{\mathrm{eff},\mathrm{L,T}} \equiv m_{\mathrm{eff},\parallel}$ and $\Omega_{\mathrm{L,T}} = \Omega_\parallel$), where $C_{\mathbf{k},l} = \mathbf{e}_{\mathbf{k},l}\cdot\bar{\bar{\mathbf{C}}}_\mathbf{k}\cdot\mathbf{e}_{\mathbf{k},l}$, which yields the eigennumbers defined by Eq. (6). Note that the frequencies of the normal modes satisfy $\omega_{-\mathbf{k},l} = \omega_{\mathbf{k},l}$.

The associated eigenvector with the normalization $\mathbf{F}_{\mathbf{k},l}^\dagger\mathbf{MF}_{\mathbf{k},l} = 1$ is given by

$$\mathbf{F}_{\mathbf{k},l} = \frac{e^{i\psi_l}}{\sqrt{2N\omega_{\mathbf{k},l}}}\begin{pmatrix}\frac{1}{\sqrt{m_{\mathrm{eff},l}\omega_{\mathbf{k},l}}}\left[\mathbf{e}_{\mathbf{k},l}e^{i\mathbf{k}\cdot\mathbf{r}_q}\right]_N \\ -i\sqrt{m_{\mathrm{eff},l}\omega_{\mathbf{k},l}}\left[\mathbf{e}_{\mathbf{k},l}e^{i\mathbf{k}\cdot\mathbf{r}_q}\right]_N\end{pmatrix}, \tag{B3}$$

where the initial phase ψ_l can be chosen at will. It is convenient to set $\psi_\perp = 0$ and $\psi_{\mathrm{L,T}} = \pi/2$, and introduce complex unit vectors $\tilde{\mathbf{e}}_{\mathbf{k},l}$ such that $\tilde{\mathbf{e}}_{\mathbf{k},l} = e^{i\psi_l}\mathbf{e}_{\mathbf{k},l}$. Evidently, $\tilde{\mathbf{e}}_{\mathbf{k},l}\cdot\tilde{\mathbf{e}}_{\mathbf{k},l}^* = 1$, and $\tilde{\mathbf{e}}_{-\mathbf{k},l}^* = \tilde{\mathbf{e}}_{\mathbf{k},l}$. In the new notation, Eq. (B3) assumes the form of Eq. (5).

Additionally, it is convenient to split the interaction factors as $C_{\mathbf{k},l} = C_{0,l} + \tilde{C}_{\mathbf{k},l}$, where $C_{0,l}$ is the limit of $C_{\mathbf{k},l}$ at $\mathbf{k}\to 0$. Evidently, $\lim_{\mathbf{k}\to 0}\tilde{C}_{\mathbf{k},l} = 0$. Then,

$$\omega_{\mathbf{k},l} = \sqrt{\tilde{\Omega}_l^2 + \frac{e^2\tilde{C}_{\mathbf{k},l}}{4\pi\varepsilon_0 m_{\mathrm{eff},l}}}, \tag{B4}$$

with $\tilde{\Omega}_l^2 = \Omega_l^2 + C_{0,l}e^2/(4\pi\varepsilon_0 m_{\mathrm{eff},l})$, which are the squares of the normal frequencies of oscillation in the long-wavelength limit: $\tilde{\Omega}_l = \lim_{\mathbf{k}\to 0}\omega_{\mathbf{k},l}$.

APPENDIX C: THE INTERACTION HAMILTONIAN OF TWO ARRAYS IN RELATIVE MOTION

To quantize H_{12} we replace $\mathbf{x}_{1,s,\alpha}$ and $\mathbf{x}_{2,q,\beta}$ in Eq. (14) by the respective operators defined consistently with Eq. (12). We note that from Eqs. (5) and (12), and the properties of the complex unit vectors $\tilde{\mathbf{e}}_{\mathbf{k},l}$, it follows that the displacement component $\hat{\mathbf{x}}_{q,l}$ of the state operator $\hat{\mathbf{F}}$ can be expressed as

$$\hat{\mathbf{x}}_{q,l} = \sqrt{\frac{\hbar}{2N}} \sum_{\omega_{\mathbf{k},l}>0} \frac{\hat{a}_{\mathbf{k},l}\tilde{\mathbf{e}}_{\mathbf{k},l} e^{i\mathbf{k}\cdot\mathbf{r}_q} + \hat{a}^\dagger_{\mathbf{k},l}\tilde{\mathbf{e}}^*_{\mathbf{k},l} e^{-i\mathbf{k}\cdot\mathbf{r}_q}}{\sqrt{m_{\mathrm{eff},l}\omega_{\mathbf{k},l}}}$$
$$= \sqrt{\frac{\hbar}{2N}} \sum_{\omega_{\mathbf{k},l}>0} \frac{(\hat{a}_{\mathbf{k},l} + \hat{a}^\dagger_{-\mathbf{k},l})\tilde{\mathbf{e}}_{\mathbf{k},l} e^{i\mathbf{k}\cdot\mathbf{r}_q}}{\sqrt{m_{\mathrm{eff},l}\omega_{\mathbf{k},l}}}. \tag{C1}$$

From here it is found that

$$\hat{H}_{12} = \frac{\hbar e^2}{8\pi\varepsilon_0} \sum_{\alpha,\beta=\perp,\mathrm{L},\mathrm{T}} \sum_{\substack{\omega_{\mathbf{k}_1,\alpha}>0 \\ \omega_{\mathbf{k}_2,\beta}>0}} \frac{C_{\mathbf{k}_1\mathbf{k}_2,\alpha\beta}(h)}{\sqrt{m_{\mathrm{eff},\alpha} m_{\mathrm{eff},\beta}\omega_{\mathbf{k}_1,\alpha}\omega_{\mathbf{k}_2,\beta}}}$$
$$\times \left(\hat{a}_{1,\mathbf{k}_1,\alpha} + \hat{a}^\dagger_{1,-\mathbf{k}_1,\alpha}\right)\left(\hat{a}_{2,\mathbf{k}_2,\beta} + a^\dagger_{2,-\mathbf{k}_2,\beta}\right), \tag{C2}$$

with $C_{\mathbf{k}_1\mathbf{k}_2,\alpha\beta}(h) = \tilde{\mathbf{e}}_{\mathbf{k}_1,\alpha} \cdot \overline{\overline{\mathbf{C}}}_{\mathbf{k}_1\mathbf{k}_2}(h) \cdot \tilde{\mathbf{e}}_{\mathbf{k}_2,\beta}$, and

$$\overline{\overline{\mathbf{C}}}_{\mathbf{k}_1\mathbf{k}_2}(h) = \frac{1}{N} \sum_{s,q} \overline{\overline{\Phi}}_{sq} e^{i\mathbf{k}_1\cdot\mathbf{r}_{1,s}} e^{i\mathbf{k}_2\cdot\mathbf{r}_{2,q}}. \tag{C3}$$

The separation $\mathbf{R}_{sq} = \mathbf{u}_{sq} R_{sq}$ between a pair of selected oscillators in the two moving arrays changes with time, and, therefore, $\overline{\overline{\Phi}}_{sq}(h) \equiv (\bar{\bar{\mathbf{I}}} - \mathbf{u}_{sq}\mathbf{u}_{sq})/R^3_{sq}$ also does. However, in the limit when the lattice period tends to zero (the continuous limit), the vector $\mathbf{v}t$ at any fixed time instant may be approximated by the nearest translation vector of the lattice, i.e., for any q there exists such q' that $\mathbf{r}_{2,q'} \approx \mathbf{r}_{2,q} + \mathbf{v}t$ and $\mathbf{R}_{sq} \approx \mathbf{r}_{2,q'} - \mathbf{r}_{1,s} + \mathbf{h} \equiv \mathbf{R}_{sq'}$. Therefore, $\overline{\overline{\mathbf{C}}}_{\mathbf{k}_1\mathbf{k}_2}(h)$ reduces to $\overline{\overline{\mathbf{C}}}_{\mathbf{k}_1\mathbf{k}_2}(h) = \delta_{\mathbf{k}_1,-\mathbf{k}_2} e^{-i\mathbf{k}_2\cdot\mathbf{v}t} \overline{\overline{\mathbf{C}}}_{\mathbf{k}_2}(h)$, with $\overline{\overline{\mathbf{C}}}_{\mathbf{k}_2}(h) = \sum_{q'} \overline{\overline{\Phi}}_{0q'}(h) e^{i\mathbf{k}_2\cdot\mathbf{R}_{0q'}}$.

Substituting these results into Eq. (C2) we obtain

$$\hat{H}_{12} = \frac{\hbar e^2}{8\pi\varepsilon_0} \sum_{\alpha,\beta=\perp,\mathrm{L},\mathrm{T}} \sum_{\omega_{\mathbf{k}}>0} \frac{C_{\mathbf{k},\alpha\beta}(h)}{\sqrt{m_{\mathrm{eff},\alpha} m_{\mathrm{eff},\beta}\omega_{\mathbf{k},\alpha}\omega_{\mathbf{k},\beta}}}$$
$$\times (\hat{a}_{1,\mathbf{k},\alpha} + \hat{a}^\dagger_{1,-\mathbf{k},\beta})(\hat{a}^\dagger_{2,\mathbf{k},\beta} + \hat{a}_{2,-\mathbf{k},\beta})\, e^{i\mathbf{k}\cdot\mathbf{v}t}, \tag{C4}$$

where we put $C_{\mathbf{k},\alpha\beta}(h) = \tilde{\mathbf{e}}_{\mathbf{k},\alpha} \cdot \overline{\overline{\mathbf{C}}}_{-\mathbf{k}}(h) \cdot \tilde{\mathbf{e}}^*_{\mathbf{k},\beta}$. Evidently, $C_{-\mathbf{k},\alpha\beta}(h) = [C_{\mathbf{k},\alpha\beta}(h)]^*$, which ensures that $\hat{H}_{12}$ is a Hermitian operator. It should be noted that because the operators associated with each array commute, the multiplication order in (C4) is irrelevant.

In the continuous limit,

$$\overline{\overline{\mathbf{C}}}_{\mathbf{k}}(h) = \frac{1}{A_\mathrm{c}} \int \frac{(\bar{\bar{\mathbf{I}}} - 3\mathbf{r}\mathbf{r}/r^2)\, e^{i\mathbf{k}\cdot\mathbf{r}}}{r^3}\, dS$$
$$= -\frac{1}{A_\mathrm{c}} \int \nabla\nabla\left(\frac{1}{r}\right) e^{i\mathbf{k}\cdot\mathbf{r}}\, dS, \tag{C5}$$

where $\mathbf{r} = \sum_\alpha x_\alpha \mathbf{e}_\alpha - h\mathbf{e}_\perp$, $\alpha = \perp,\mathrm{L},\mathrm{T}$, $r \equiv |\mathbf{r}|$, A_c is the unit cell area, and the integration is done over the plane $x_\perp = 0$ (the array plane). From Eq. (C5), assuming $h > 0$,

$$\overline{\overline{\mathbf{C}}}_{\mathbf{k}}(h) = \frac{2\pi}{A_\mathrm{c}} \frac{\mathbf{K}\mathbf{K}}{|\mathbf{k}|} e^{-|\mathbf{k}|h} = \frac{4\pi|\mathbf{k}|e^{-|\mathbf{k}|h}}{A_\mathrm{c}} \tilde{\mathbf{e}}_{\mathbf{k},-}\tilde{\mathbf{e}}^*_{\mathbf{k},+}, \tag{C6}$$

where $\mathbf{K} = \mathbf{k} + i|\mathbf{k}|\mathbf{e}_{\mathbf{k},\perp}$ and $\tilde{\mathbf{e}}_{\mathbf{k},\pm} = (\tilde{\mathbf{e}}_{\mathbf{k},\mathrm{L}} \pm \tilde{\mathbf{e}}_{\mathbf{k},\perp})/\sqrt{2}$. The vectors $\tilde{\mathbf{e}}_{\mathbf{k},\pm}$ satisfy $\tilde{\mathbf{e}}^*_{-\mathbf{k},\pm} = \tilde{\mathbf{e}}_{\mathbf{k},\pm}$, $\tilde{\mathbf{e}}_{\mathbf{k},\pm}\cdot\tilde{\mathbf{e}}^*_{\mathbf{k},\pm} = 1$, $\tilde{\mathbf{e}}_{\mathbf{k},\pm}\cdot\tilde{\mathbf{e}}^*_{\mathbf{k},\mp} = 0$, and $\tilde{\mathbf{e}}_{\mathbf{k},\pm} = -\tilde{\mathbf{e}}^*_{\mathbf{k},\mp}$.

It is evident that the interaction factors $C_{\mathbf{k},\alpha\beta} = \tilde{\mathbf{e}}_{\mathbf{k},\alpha} \cdot \overline{\overline{\mathbf{C}}}_{-\mathbf{k}}(h) \cdot \tilde{\mathbf{e}}^*_{\mathbf{k},\beta}$ can be understood as the matrix elements of $\overline{\overline{\mathbf{C}}}_{-\mathbf{k}}(h)$ in the complex basis $\mathbf{e}_{1,2,3} = \tilde{\mathbf{e}}_{\mathbf{k},\perp,\mathrm{L},\mathrm{T}}$. Using (C6) and performing the necessary calculations we find that $C_{\mathbf{k},\alpha\beta}(h) = 2\pi A_\mathrm{c}^{-1}|\mathbf{k}|\, e^{-|\mathbf{k}|h} g_{\alpha\beta}$, where $g_{\alpha\beta}$ is given by

$$[g_{\alpha\beta}]_{3\times3} = \begin{pmatrix} -1 & -1 & 0 \\ 1 & 1 & 0 \\ 0 & 0 & 0 \end{pmatrix}, \tag{C7}$$

from which it is seen that the T-polaritons do not contribute to the interaction Hamiltonian.

It is convenient to introduce the normalized interaction factor $c_{\mathbf{k},\alpha\beta} = C_{\mathbf{k},\alpha\beta}(h)/\sqrt{|\tilde{C}_{\mathbf{k},\alpha}\tilde{C}_{\mathbf{k},\beta}|}$ (where $\alpha = \perp,\mathrm{L}$, $\beta = \perp,\mathrm{L}$), with $\tilde{C}_{\mathbf{k},\alpha}$ being the interaction constant defined in Appendix B above Eq. (B4). In Appendix D we prove that in the continuous limit $\tilde{C}_{\mathbf{k},\alpha} = C_{\mathbf{k},\alpha\alpha}(0)$, and thus the normalized interaction factor equals $c_{\mathbf{k},\alpha\beta} = g_{\alpha\beta}\exp(-|\mathbf{k}|h)$. Then, using the formula $|\tilde{C}_{\mathbf{k},\alpha}| = (4\pi\varepsilon_0 m_{\mathrm{eff},\alpha}/e^2)|\omega^2_{\mathbf{k},\alpha} - \tilde{\Omega}^2_\alpha|$ [Eq. (B4)], we obtain from Eq. (C4) the interaction Hamiltonian of Sec. III [Eq. (15)].

The single-component form of the interaction dyadic $\overline{\overline{\mathbf{C}}}_{\mathbf{k}}(h)$ [Eq. (C5)] suggests that the interaction Hamiltonian (15) can be further simplified if one changes to a suitable basis in the subspace $\mathbf{F}_{\mathbf{k},\mathrm{L}} \oplus \mathbf{F}_{\mathbf{k},\perp}$. Below we show that in the degenerate case when $\omega_{\mathbf{k},\perp} = \omega_{\mathbf{k},\mathrm{L}} = \omega_\mathbf{k}$ and $m_{\mathrm{eff},\perp} = m_{\mathrm{eff},\parallel} = m_\mathrm{eff}$ such a basis is essentially a basis of SPP-like modes.

Let us note that in our model the degeneracy conditions can be fulfilled only approximately, when $\omega_\mathbf{k} \approx \mathrm{const}(\mathbf{k})$, which implies that $|\tilde{C}_{\mathbf{k},l}| \ll |C_{0,l}|$, $l = \perp,\mathrm{L}$. Under these conditions the L- and $\perp$-polarized modes strongly hybridize. Indeed, in the degenerate case one may introduce a new orthonormal basis $\mathbf{F}_{\mathbf{k},\pm} = (\mathbf{F}_{\mathbf{k},\mathrm{L}} \pm \mathbf{F}_{\mathbf{k},\perp})/\sqrt{2}$. When $\omega_{\mathbf{k},\perp} = \omega_{\mathbf{k},\mathrm{L}}$ and $m_{\mathrm{eff},\perp} = m_{\mathrm{eff},\parallel}$ the components of $\mathbf{F}_{\mathbf{k},\pm}$ are collinear with the vectors $\tilde{\mathbf{e}}_{\mathbf{k},\pm} = (\tilde{\mathbf{e}}_{\mathbf{k},\mathrm{L}} \pm \tilde{\mathbf{e}}_{\mathbf{k},\perp})/\sqrt{2}$, through which the interaction dyadic (C5) is expressed. Thus, the electric dipole moment associated with these polarization waves, $\mathbf{d}_{\mathbf{k},\pm} = e\mathbf{x}_{\mathbf{k},\pm}$ [here, $\mathbf{x}_{\mathbf{k},\pm}$ is the displacement component of $\mathbf{F}_{\mathbf{k},\pm}$ as in Eq. (B1)], is such that $\mathbf{d}_{\mathbf{k},\pm} \propto \tilde{\mathbf{e}}_{\mathbf{k},\pm}$.

In this basis the interaction Hamiltonian (C4) assumes the simplest form

$$\hat{H}_{12} = \frac{e^2\hbar}{8\pi\varepsilon_0} \sum_{\omega_\mathbf{k}>0} \frac{C_{\mathbf{k},\pm}(h)}{m_\mathrm{eff}\omega_\mathbf{k}} e^{i\mathbf{k}\cdot\mathbf{v}t}$$
$$\times (\hat{c}_{1,\mathbf{k},-} + \hat{c}^\dagger_{1,-\mathbf{k},-})(\hat{c}^\dagger_{2,\mathbf{k},+} + \hat{c}_{2,-\mathbf{k},+}), \tag{C8}$$

where $C_{\mathbf{k},\pm}(h) = \tilde{\mathbf{e}}_{\mathbf{k},-} \cdot \overline{\overline{\mathbf{C}}}_{-\mathbf{k}}(h) \cdot \tilde{\mathbf{e}}^*_{\mathbf{k},+} = 4\pi A_\mathrm{c}^{-1}|\mathbf{k}|e^{-|\mathbf{k}|h}$ and $\hat{c}_{l,\mathbf{k},\pm} = (\hat{a}_{l,\mathbf{k},\mathrm{L}} \pm \hat{a}_{l,\mathbf{k},\perp})/\sqrt{2}$, $l = 1,2$, are the annihilation operators in the new basis. Note that the interacting modes are just the "−" modes of the first slab and the "+" modes of the second slab.

It is possible to associate the "±" modes with SPPs at the surfaces of a plasmonic slab. Indeed, in such SPPs the polarization vector $\mathbf{P} \approx \mathbf{P}_{\mathbf{k}} e^{i\mathbf{k}\cdot\mathbf{r}} e^{|\mathbf{k}|(\mathbf{n}\cdot\mathbf{r})}$ (here $\mathbf{n}$ is the outward unit normal to a surface, and $\mathbf{k}$ is the in-plane component of the wave vector, $|\mathbf{k}| \gg \omega_{\mathbf{k}}/c$) is such that $(\mathbf{n}\cdot\mathbf{P}_{\mathbf{k}}) \approx -i(\mathbf{k}\cdot\mathbf{P}_{\mathbf{k}})/|\mathbf{k}|$. This holds because inside the slab $\nabla\cdot\mathbf{P} = 0$. For the two surfaces of the slab, $\mathbf{n}_1 = -\mathbf{n}_2$, therefore, for the SPPs localized at these surfaces, $\mathbf{P}_{\mathbf{k}} \propto i\mathbf{k}/|\mathbf{k}| + \mathbf{n}_{1,2} = \tilde{\mathbf{e}}_{\mathbf{k},\mathrm{L}} \pm \tilde{\mathbf{e}}_{\mathbf{k},\perp}$, i.e., $\mathbf{P}_{\mathbf{k}} \propto \mathbf{d}_{\mathbf{k},\pm}$. Therefore, the modes $\mathbf{F}_{\mathbf{k},\pm}$ are fully analogous to the SPPs at the surfaces of a plasmonic slab. On the other hand, the modes $\mathbf{F}_{\mathbf{k},\mathrm{L}} = (\mathbf{F}_{\mathbf{k},+} + \mathbf{F}_{\mathbf{k},-})/\sqrt{2}$ and $\mathbf{F}_{\mathbf{k},\perp} = (\mathbf{F}_{\mathbf{k},+} - \mathbf{F}_{\mathbf{k},-})/\sqrt{2}$ can be understood as the result of hybridization of such SPPs, i.e., as the SR SPP and LR SPP modes of a plasmonic slab.

APPENDIX D: RELATION BETWEEN $\tilde{C}_{\mathbf{k},\alpha}$ AND $C_{\mathbf{k},\alpha\alpha}(h)$ IN THE CONTINUOUS LIMIT

Let us consider the lattice sum $\tilde{C}_{\mathbf{k},\alpha} = C_{\mathbf{k},\alpha} - C_{0,\alpha}$. It can be written as

$$\tilde{C}_{\mathbf{k},\alpha} = \sum_{q\neq 0} \frac{1 - 3(\mathbf{e}_\alpha\cdot\mathbf{u}_{0q})^2}{R_{0q}^3}(\cos\mathbf{k}\cdot\mathbf{R}_{0q} - 1). \tag{D1}$$

One may notice that in a dense lattice (i.e., when $k\sqrt{A_c} \ll 1$, with A_c being the unit cell area) the terms with $\mathbf{k}\cdot\mathbf{R}_{0q} \ll 1$ may contribute less to the value of the sum than the distant terms. Namely, we may write Eq. (D1) as

$$\sum_{q\neq 0}\Phi_{q,\alpha} = \sum_{R_{0q}<R_\Sigma}\Phi_{q,\alpha} + \sum_{R_{0q}\geqslant R_\Sigma}\Phi_{q,\alpha}, \tag{D2}$$

where $kR_\Sigma \ll 1$, and $\Phi_{q,\alpha} = [1 - 3(\mathbf{e}_\alpha\cdot\mathbf{u}_{0q})^2](\cos\mathbf{k}\cdot\mathbf{R}_{0q} - 1)/R_{0q}^3$. Expressing $\cos\mathbf{k}\cdot\mathbf{R}_{0q} - 1 = -2\sin^2\frac{\mathbf{k}\cdot\mathbf{R}_{0q}}{2}$ and using the inequality $|\sin x| \leqslant |x|$, we obtain that

$$\left|A_c\sum_{R_{0q}<R_\Sigma}\Phi_{q,\alpha}\right| \leqslant A_c\sum_{R_{0q}<R_\Sigma}\frac{(\mathbf{k}\cdot\mathbf{R}_{0q})^2}{R_{0q}^3} \leqslant k^2A_c\sum_{R_{0q}<R_\Sigma}\frac{1}{R_{0q}}. \tag{D3}$$

From here, using that $\min(R_{0q}) \sim \sqrt{A_c}$ and that there are about $\pi R_\Sigma^2/A_c$ terms in the summation, we obtain

$$\left|A_c\sum_{R_{0q}<R_\Sigma}\Phi_{q,\alpha}\right| \lesssim (\pi k)(kR_\Sigma)\left(\frac{R_\Sigma}{\sqrt{A_c}}\right).$$

Because in the continuous limit we may always ensure that $R_\Sigma \gg \sqrt{A_c}$, while $kR_\Sigma \ll \sqrt{A_c}/R_\Sigma$, the summation over $R_{0q} < R_\Sigma$ may be neglected in (D2) and the summation over $R_{0q} \geqslant R_\Sigma$ replaced by integration. Thus, in the continuous limit,

$$A_c\sum_q\Phi_{q,\alpha} \approx \int_{r\geqslant R_\Sigma}\frac{(1 - 3r_\alpha^2/r^2)(\cos\mathbf{k}\cdot\mathbf{r} - 1)}{r^3}\,dS.$$

Next, because this integral does not have a singularity at $r = 0$, we may as well include the region $r < R_\Sigma$ into the integration (the contribution of this region is on the order of $k^2R_\Sigma/2$) and obtain that in the continuous limit

$$\tilde{C}_{\mathbf{k},\alpha} = \frac{1}{A_c}\int\frac{(1 - 3r_\alpha^2/r^2)(\cos\mathbf{k}\cdot\mathbf{r} - 1)}{r^3}\,dS = \frac{1}{A_c}\int\left[\frac{(1 - 3r_\alpha^2/r^2)e^{i\mathbf{k}\cdot\mathbf{r}}}{r^3} - \frac{(1 - 3r_\alpha^2/r^2)}{r^3}\right]dS. \tag{D4}$$

Next, for any finite $h > 0$ and $\mathbf{k} = \mathbf{0}$ we get from Eq. (C5) that

$$\int\frac{(1 - 3r_\alpha^2/r^2)}{r^3}\,dS = \mathbf{e}_{\mathbf{k},\alpha}\cdot\overline{\overline{\mathbf{C}}}_{\mathbf{k}}(h)\cdot\mathbf{e}_{\mathbf{k},\alpha} = 0.$$

Therefore, we may write based on Eq. (D4) that

$$\lim_{h\to 0}(\mathbf{e}_{\mathbf{k},\alpha}\cdot\overline{\overline{\mathbf{C}}}_{\mathbf{k}}(h)\cdot\mathbf{e}_{\mathbf{k},\alpha}) = \frac{1}{A_c}\lim_{h\to 0}\int\frac{(1 - 3r_\alpha^2/r^2)(e^{i\mathbf{k}\cdot\mathbf{r}} - 1)}{r^3}\,dS = \tilde{C}_{\mathbf{k},\alpha}. \tag{D5}$$

From here, because, $\mathbf{e}_{\mathbf{k},\alpha}\cdot\overline{\overline{\mathbf{C}}}_{\mathbf{k}}(0)\cdot\mathbf{e}_{\mathbf{k},\alpha} = \tilde{\mathbf{e}}_{\mathbf{k},\alpha}\cdot\overline{\overline{\mathbf{C}}}_{-\mathbf{k}}(0)\cdot\tilde{\mathbf{e}}^*_{\mathbf{k},\alpha}$ we get that $\tilde{C}_{\mathbf{k},\alpha} = C_{\mathbf{k},\alpha\alpha}(0)$.

In Fig. 5 we compare the interaction factors $\tilde{C}_{\mathbf{k},\alpha}$ computed numerically by direct summation of the absolutely convergent series (D1) with the same obtained in the continuous approximation (D5). One may see that the agreement is quite good even for arrays that are far from the continuous limit $ka \to 0$. We conclude that this approximation may work quite well already for $ka \lesssim 0.5$.

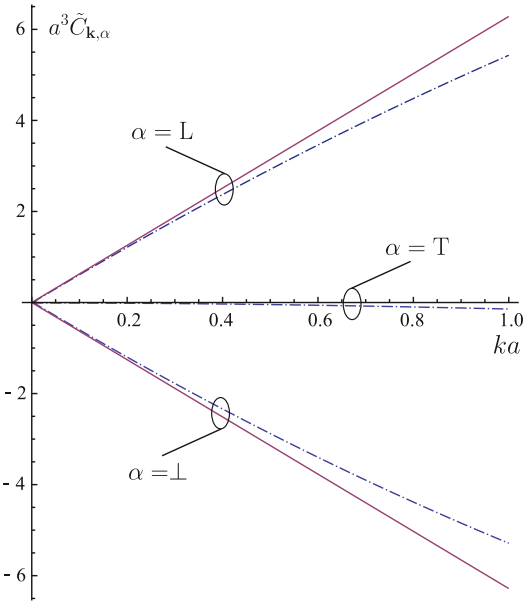

FIG. 5. (Color online) Normalized interaction factors $a^3\tilde{C}_{\mathbf{k},\alpha} = a^3(C_{\mathbf{k},\alpha} - C_{0,\alpha})$, $\alpha = \perp$,L,T, computed numerically by direct summation of the series (D1) over a 600×600 element square-cell lattice (dash-dotted lines), and analytically by using the continuous approximation (D5) (solid lines), as functions of the normalized in-plane wave number ka, where a is the lattice constant.

[1]E. V. Teodorovich, Proc. R. Soc. London Ser. A **362**, 71 (1978).
[2]L. S. Levitov, Europhys. Lett. **8**, 499 (1989).
[3]V. Mkrtchian, Phys. Lett. A **207**, 299 (1995).
[4]J. B. Pendry, J. Phys.: Condens. Matter **9**, 10301 (1997).
[5]A. I. Volokitin and B. N. J. Persson, J. Phys.: Condens. Matter **11**, 345 (1999).
[6]A. I. Volokitin and B. N. J. Persson, Rev. Mod. Phys. **79**, 1291 (2007).
[7]T. G. Philbin and U. Leonhardt, New J. Phys. **11**, 033035 (2009).
[8]J. B. Pendry, New J. Phys. **12**, 033028 (2010).
[9]U. Leonhardt, New J. Phys. **12**, 068001 (2010).
[10]J. B. Pendry, New J. Phys. **12**, 068002 (2010).
[11]A. I. Volokitin and B. N. J. Persson, New J. Phys. **13**, 068001 (2011).
[12]J. S. Høye and I. Brevik, Europhys. Lett. **91**, 60003 (2010).
[13]G. Barton, New J. Phys. **12**, 113044 (2010).
[14]G. Barton, New J. Phys. **12**, 113045 (2010).
[15]A. Manjavacas and F. J. García de Abajo, Phys. Rev. Lett. **105**, 113601 (2010).
[16]A. Manjavacas and F. J. García de Abajo, Phys. Rev. A **82**, 063827 (2010).
[17]A. I. Volokitin and B. N. J. Persson, Phys. Rev. Lett. **106**, 094502 (2011).
[18]A. I. Volokitin and B. N. J. Persson, Phys. Rev. B **83**, 241407 (2011).
[19]G. Barton, New J. Phys. **13**, 043023 (2011).
[20]G. Barton, J. Phys.: Condens. Matter **23**, 355004 (2011).
[21]M. F. Maghrebi, R. L. Jaffe, and M. Kardar, Phys. Rev. Lett. **108**, 230403 (2012).
[22]R. Zhao, A. Manjavacas, F. J. García de Abajo, and J. B. Pendry, Phys. Rev. Lett. **109**, 123604 (2012).
[23]S. I. Maslovski, Phys. Rev. A **84**, 022506 (2011).
[24]J. J. Hopfield, Phys. Rev. **112**, 1555 (1958).
[25]S. J. Smith and E. M. Purcell, Phys. Rev. **92**, 1069 (1953).
[26]P. A. Cherenkov, Dokl. Akad. Nauk SSSR **2**, 451 (1934).
[27]D. E. Fernandes, S. I. Maslovski, and M. G. Silveirinha, Phys. Rev. B **85**, 155107 (2012).
[28]M. Currie and R. Gould, Proc. IRE **48**, 1960 (1960).
[29]W. H. Louisell, A. Yariv, and A. E. Siegman, Phys. Rev. **124**, 1646 (1961).
[30]J. P. Gordon, W. H. Louisell, and L. R. Walker, Phys. Rev. **129**, 481 (1963).
[31]Because the plasmons are generated in pairs, the threshold for plasmon generation is at $v = 2v_{\rm ph}$. In the Cherenkov effect the threshold is at $v = v_{\rm ph}$.
[32]S. I. Maslovski and M. G. Silveirinha, Phys. Rev. A **84**, 062509 (2011).
[33]M. G. Silveirinha and S. I. Maslovski, Phys. Rev. A **86**, 042118 (2012).
[34]D. Sarid, Phys. Rev. Lett. **47**, 1927 (1981).